

# 1. INTRODUCTION

## 1.1 General

Before introducing the actual problem hypothesis, it is useful to present the background perspective illustrating why zoned rockfill dam structure is taken as the case in this research work (thesis). A chain of issues on the need of multipurpose dam projects in Nepal and the BMP as a case followed by the opportunities and challenges to develop rockfill dams in Nepal, especially in relation to its high seismicity, are discussed in sections 1.1.1 and 1.1.2.

### 1.1.1 Need of multipurpose dam projects in Nepal and the BMP

Nepal is the Himalayan country. It has a huge hydro potential. In Nepalese rivers, there is considerable variation in flow during monsoon and non-monsoon seasons and as the run-off-river plants are usually designed for the flow available for only 50% of the year, there is a huge wastage of water power during the monsoon season and deficiency in non-monsoon. This could be utilized by storage type plants by constructing the dam structures. At present, 93 dam-sites have been identified and 66 of these are found economically feasible with a total generating capacity of about 42,000 MW. However, the present situation is that Nepal has developed only approximately 600 MW of hydropower. Therefore, bulk of the economically feasible generation has not been realized yet. Demand forecast chart of NEA shows that by 2015 AD, the usual electricity demand will be about 1200 MW. That means new plants having a total installed capacity of around 600 MW should be installed within that time to meet the increasing demand. However, no large project has been started yet. Unfortunately, Nepalese are facing the load shedding of more than 40 hours a week in the month of January/February and also for some hours even in the month of July/August. Although the storage type power plants require huge initial capital investment, they are the only means for the efficient and controlled use of the available water. Nepal's only reservoir power scheme, so far, built in 1982 is the zoned rockfill dam built over a medium size river called Kulekhani River. The plant has a total capacity of 92 MW (I and II) and is absorbing the seasonal as well the daily peaks of the Nepalese power system. So, to cope with the

increasing power demand and to absorb the peaks, other storage type plants should be commissioned. [13]

Nepal has water resources equivalent to 200 billion cubic meters as surface and 12 billion cubic meters as ground water surplus for development of the 1.80 million hectares of available land for irrigation. Out of this potential irrigable land with 68% share in Terai belt, irrigation infrastructure has been developed for over 1.09 million hectares. Overall net irrigated areas in summer and winter are about 72.4% and 33.3% respectively. Large-scale irrigation is feasible in the Terai plains where large, extensive and more uniform land is available. The most possible run-of-the-river projects have already been taken up for development though intensive infrastructure development and quality water management is lacking. Multipurpose dam projects which have high potentials for year-round irrigation in the Terai are awaiting implementation. Moreover, the whole of the Terai is inundated in the country in the months of monsoon. A storage plant can play important role for the control of flood hazard. [13]

In summary, if properly planned and managed, the development of Nepal's storage potential could yield tremendous benefits to Nepal and its neighbors in the form of hydropower generation, flow augmentation for downstream irrigation and flood control during monsoon. Navigation and recreation could be other important aspects of multipurpose projects.

Bagmati multipurpose dam site is one of the attractive storage sites identified in Nepal.

Bagmati Multipurpose Project (BMP) was identified in the late sixties by Nippon Koei Co. Ltd., Japan during the course of UNDP/FAO irrigation development study in the central and eastern Terai plain. Studies by Nippon Koei in 1971 suggested a multipurpose project with a major dam and reservoir located in the Siwalik Hills, a 70 MW power station at the toe of dam and irrigation of about 120,000 hectares of agricultural land in the nearby Terai. In 1977, the German Mission for Water Resources Development in Nepal carried out an identification and appraisal study of the requested projects, which included also the BMP. Consequently, in January 1979, the Phase-I work for feasibility study of BMP was started by the government of Nepal in assistance of the Federal Republic of Germany. In 1981 was

produced the final report suggesting a 117 m high zoned rockfill dam having the potential of 140 MW of power generation and 120,000 hectares of irrigation development and also the flood retention of 7 m head above the full supply level. [1]

It is reported<sup>16</sup> that due to different limitations, Department of Irrigation undertook Bagmati Irrigation Project (BIP) with construction of a R-O-R barrage for irrigating 68,000 ha through splitting onto two stages (stage-I for 30,000 ha and stage-II for 38,000 ha). The canals were designed to accommodate higher discharge with the expectation that BMP high dam would be constructed upstream of the barrage in future.

The updated study of BMP<sup>16</sup> in 1999 has also suggested that the project is feasible. The analysis and design of the same project was also reviewed in the IOE, Pulchowk Campus as the B.E. final year project work<sup>13</sup> in 2004.

### **1.1.2 Nepal's high seismicity and implication to rockfill dams**

The Himalaya evolved as a consequence of collision of the Asian and Indian continents. As the Indian continent persistently pushes northwards (underthrusting) at the rate of around 5 cm per year, the Himalayan faults remain tectonically and seismically active. Many of the faults and thrusts of the Himalaya have given rise to earthquakes, some of very high magnitude (M 8.5 or higher) from one end to the other of the entire 2400 km long section.

[17]

In the following are cited some examples of the ground motion parameters adopted at different proposed dam sites of the Himalaya revealing its high seismicity.

For the West-Seti Dam<sup>53</sup> site, Nepal, the peak horizontal acceleration with the return period of 500 years was obtained to be 445 gals by Weibull's direct statistical results and 400 gals by Cornell's method.

For Chisapani High Dam<sup>52</sup>, Nepal, the peak acceleration was estimated to be 0.4 g for the maximum credible earthquake; 0.4 g corresponding to M = 7.0 and an epicentral distance of 10 km.

During the controversy raised regarding the inadequate design of the Tehri Dam in UP, India, the design PGA estimated showed that the 84<sup>th</sup> percentile estimate at a site representative of that of Tehri Dam would be 0.75 g. [17]

International experiences with the rockfill dams such as Coyote Lake Dam (USA), Makio Dam (Japan), La Villita Dam (Mexico), Anbuklao Dam (Philippines) etc conclude that the rockfill dams have high seismic resistance. [39]

From the point of view of seismic resistance as well as the availability of local construction materials and relatively easy construction technology, the zoned rockfill dams are most suitable in context of Nepal. However, development of analytical and experimental capabilities for the analysis and design of such large and very important structures should not be underestimated.

The structural analysis of dams, in overall, requires proper assessment of earthquake ground motion and the resulting seismic forces including hydrodynamic loads, accurate modeling and analysis techniques and the judicial interpretation of the results. In fact, a rockfill dam as a whole is very complicated in itself and its actual behavioral research needs physical model testing and an integrated effort of different areas of civil engineering such as water resources, material science, geotechnical and structural engineering. Some developed countries have formulated a great deal of design guidelines for the analysis, design and construction of such structures, though, looking minutely, a dam in itself has some unique features and needs indigenous research.

The structural research in the areas of buildings and bridges in Nepal has relatively advanced much but there, to the best information available, has been even no initiation in the area of dam structures, especially from the point of view of structural modeling and analysis. The huge potential downstream benefits of multipurpose dam projects should not lie in shade because of probable downstream hazard due to the failure of dams, in any case. In this context, it is both the matter of aptitude and the nation's necessity of the indigenous research and development in the area of high dams (zoned rockfill dam as the most suitable case) that piloted to choose this area of research.

## 1.2 Problem and issues

The safety of dams during earthquakes is extremely important because failure of such structure may have disastrous consequences to life and property. It is therefore necessary to develop the capability of evaluating the adequacy of a given design against a particular ground motion. It is evident that an accurate analytical procedure would be one of the essential tools for such an evaluation. [6]

The structural analysis and hence the concepts involved in analysis differ with the type of dam. Regarding zoned rockfill dam, the most suitable type for Nepal as stated earlier, the structural analysis is relatively complex in the sense it is really very difficult to assess the properties of geomaterials that exactly simulate the real in-situ condition and, obviously, the analysis must consider the effects of reservoir on the embankment, an aspect which does not arise in structures on land.

Having reviewed the design reports of some important existing and proposed zoned rockfill dam in Nepal such as the final design report of Kulekhani High Dam<sup>10</sup> and the feasibility level report of the proposed Bagmati Multipurpose High Dam Project<sup>1</sup>, the two important observations were noted. First, the crest elevation is determined in consideration of the safety against overtopping due to design flood; the hydraulic seepage and piping conditions are checked and the stability of dam is analyzed for different loading cases/stages such that the specified factors of safety are not exceeded, for this the limiting equilibrium of some trial slope wedges are checked. Second, the earthquake effect is incorporated in the above design by pseudo-static approach taking some seismic coefficients to account for the earthquake induced inertial forces and dynamic water pressure.

These observations feel some important issues left to be addressed.

The traditional empirical method of limit equilibrium has several theoretical flaws; particularly it does not give any information about the deformations or about the stresses in the body of the embankment, but excessive deformations and stresses can cause loss of freeboard and cracks which are likely to be the cause of failures. [23]

That is, in the conventional method of stability analysis of dams, a sliding surface is assumed and a quantitative estimate of the factor of safety is obtained by examining the equilibrium conditions at incipient failure and comparing the strength necessary to maintain limiting equilibrium with the available strength of the fill material on the entire surface. These procedures indicate the factor of safety of the dam with respect to instability but provide no information regarding the deformations of the dam. In recent years, however, there has been a growing realization of the need to determine the stress distribution and deformations inside a dam section. [47]

Again, the static method concerns only a particular aspect of the behavior of the rockfill dam with respect to an earthquake. The problem of the seismic behavior of this type of dam is more complex because of the very nature of the material. Therefore it is essential to design the zoned rockfill dams by the dynamic method. [23]

It is noteworthy to quote here the conclusion of the 13<sup>th</sup> international conference on large dams in 1979 that: “During earthquake resistant design of large dams or of important dams built in areas with high seismicity ( $PGA > 0.2 g$ ), an appropriate dynamic analysis should be carried out with data as detailed as possible.” [27]

Therefore, it is really surprising why, despite such international awareness that time, the dynamic methods were overlooked for the design of large and important zoned dams that were proposed and constructed in the highly seismic zones of Nepal. The present research is based on this query and aims at carrying out the dynamic analysis of the traditionally designed zoned rockfill type dam to evaluate its seismic performance.

In applying dynamic analysis to fill dams, the Finite Element Method (FEM) is employed which can provide solutions to any desired accuracy and can take into account irregular geometry, complex boundary conditions and material behaviour which are not possible with other analytical methods such as finite difference method. Researchers have developed many finite element computer programs for the dynamic analysis of embankment dams such as SHAKE, QUAD-4, FLUSH, STRAIN, FORCE, DIANA, ANSYS, FLAC, PROCESS etc. Some of the codes are such that they can fully incorporate the complex nonlinear plasticity

constitutive models and hence more accurate and reliable estimates of stresses and deformations can be obtained. [20]

To be specific in this broad area of finite element dynamic analysis of zoned rockfill dams, structural modeling and seismic deformation analysis are focused in this thesis. Regarding the finite element modeling of fill dams, many past researches have simply taken the assumption of foundation to be rigid. But the fixed boundary condition imposed at the base does not allow the stresses to be transferred to the foundation. In fact, it is not so in reality. Taking a part of foundation in modeling means, structurally, to incorporate the flexibility of foundation. Some researches are found to take some part of foundation in the model but do not mention exactly about how much part of the foundation is to be considered. Thus, it is required to address this problem. Regarding the dynamic analysis, deformation analysis may be of greatest interest in the case of embankment dams for a number of reasons. The most important of all is that the excessive settlements can lead to the loss of freeboard and danger of overtopping which may cause an embankment dam to collapse completely. It is very important to evaluate how much an embankment dam suffers structural deformations when excited by a particular ground motion induced by the prescribed earthquake. Therefore, these are the two major issues that the present research aims to address.

### **1.3 Objectives**

In overall, this research aims at carrying out the dynamic analysis using finite element procedures of a zoned rockfill dam which was designed by the conventional empirical methods. The high dam proposed for the Bagmati Multipurpose Project (BMP), Nepal is taken as a typical case. In particular, the following are the two major objectives that would correspondingly address the problem and issues floated earlier.

- i) To investigate the geometry of foundation to be taken for the finite element modeling of a given dam.
- ii) To evaluate the crest settlement of a given zoned rockfill dam due to given ground motion to evaluate its safety.

## **1.4 Methodology followed**

As per the first objective, the geometry of the part of foundation to be taken in the numerical modeling of the dam has been fixed based on the 'stress criteria'. The effective part of the foundation is assessed by trial procedure such that, under the self weight load of the dam embankment, the lowest pressure bulb of vertical stress in foundation obtained from the finite element analyses comes out to have practically negligible value.

Regarding the second objective, the safety via crest settlement is assessed by simplified analytical method. In fact, rigorous non-linear dynamic analysis is anticipated to accurately estimate the crest settlement of a fill dam. However, due to constraints imposed by the limited time and knowledge to develop such codes, semi-empirical approach is followed utilizing the available general purpose structural software package, SAP 2000. The linear direct integration time-history analysis is performed to determine the peak crest acceleration response of the fill dam. Then, corresponding to the ratio of yield acceleration to this peak response acceleration, the permanent displacement (settlement) of the crest is evaluated following the chart developed based on Newmark's slope stability analysis procedure. This method of employing two separate processes to predict the potential permanent settlement of the dam is given the name of 'decoupled deformation analysis'.

Before proceeding to the dynamic seismic analysis, the free vibration analysis and the initial static analysis are performed to develop basic idea on the performance of the finite element models exercised.

## **1.5 Scope and limitations**

A rockfill dam structure is very complicated in itself and its accurate structural analysis needs some advanced knowledge on soil mechanics and rock mechanics. However, the present research focuses on modeling and analysis from the point of view of structural engineering and follows the simplified techniques while dealing with other related areas. Some specific points regarding the scope and limitation of this research work are listed below.



- i) Single embankment-geometry (BMP dam), derived already as per the conventional empirical design procedure, is adopted.
- ii) Effective foundation part to be taken for numerical modeling is assessed based only on the criteria of vertical stresses due to self weight load of the embankment.
- iii) The foundation below the rock line is assumed impervious and homogeneous.
- iv) The interactions at discontinuity such as core-shell, dam-foundation and reservoir-dam are not modeled.
- v) No test for material characteristics including constitutive laws is undertaken; material properties are taken from past reports and assumed from literatures, if not available.
- vi) Analyses are carried out only for the stages of end-of-construction, and end-of-impoundment at the very early life; with reservoir at top water level. At early life, no sedimentation is assumed at the upstream face.
- vii) Single earthquake ground motion (N-S and Vertical acceleration components of 1940 Imperial Valley El-Centro earthquake) is taken.
- viii) Hydrodynamic loads and the virtual added masses are worked out simply based on Zangar's formulation as per the recommendation of IS-guideline<sup>22</sup>, the only design guideline for fill dams available to us.
- ix) Linear Time history analysis is carried out using direct integration method based on Wilson's incremental algorithm, which is inbuilt in SAP2000.
- x) The phenomena such as drawdown and cavitation are not considered.
- xi) No investigation for liquefaction is made.
- xii) Reservoir-triggered seismicity<sup>21</sup> is neglected.

## **1.6 Organization of thesis**

The main body of this thesis is divided into seven chapters, and they almost reflect the sequence of the progress followed by. Chapter 1 gives the general idea on the importance of dam structures, especially the zoned rockfill dams, to Nepal and the relevance of the present research work. It briefs on the objectives and scope of the investigation on the zoned rockfill dam of the proposed Bagmati Multipurpose Project of Nepal that the present research aims at. Chapter 2 describes the literatures reviewed on the various aspects of the finite element

dynamic analysis of fill dams. Chapter 3 is allocated for the numerical modeling, which describes on geometry of dam-foundation system and different models exercised, the finite element mesh and the various material characteristics and loads modeled. Chapter 4 devotes to the numerical analysis of the model worked out in chapter 3. Here, though the focus is on the direct integration time history analysis, the free vibration analysis and initial static deformation analysis are carried out to create acquaintance with the models so exercised. Chapter 5 contains the interpretation of the results and also includes a great deal of parametric investigations on free vibration analysis and initial static deformation analysis to justify the results. The conclusions thus derived from this investigation are given in chapter 6. A great deal of potential extensions to the present research are explored which are recommended in Chapter 7 for future works.

## 2. LITERATURE REVIEW

### 2.1 General

The numerical methods for seismic analysis for fill dams may be categorized as shown in figure 2.1. [2]

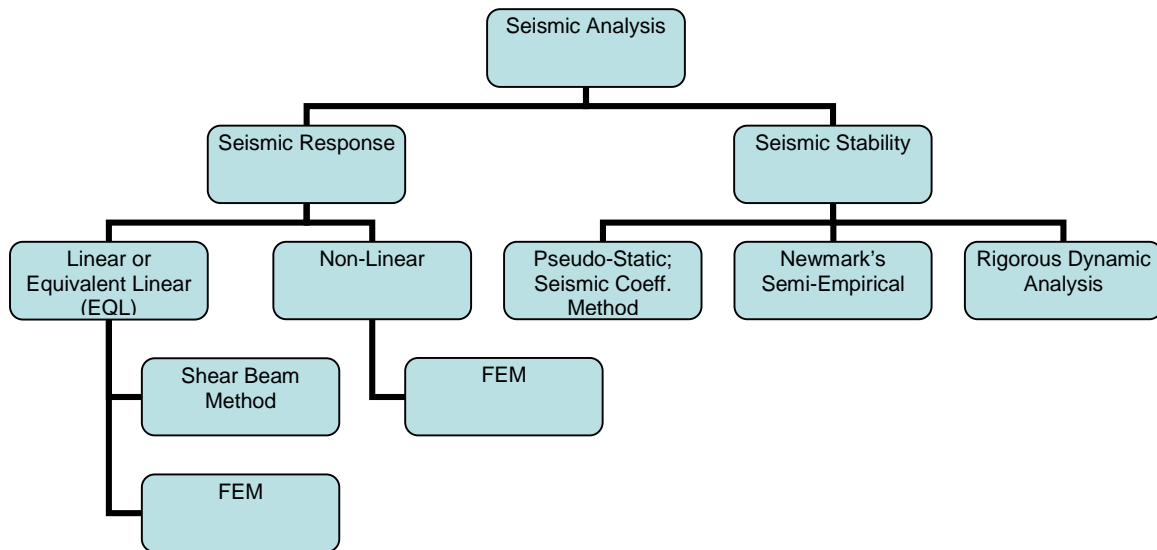


Figure 2.1: Numerical methods for seismic analysis of fill dams

From vibrational point of view, the simplest model of an earth and a rockfill dam is a two-dimensional wedge shaped shear beam. In formulation of the model, displacement of the dam is allowed only in the horizontal direction, and a uniform displacement is assumed for a horizontal plane with the same height from the bottom. [39]

In applying dynamic analysis to fill dams, the shear vibration theory was first studied as a method for arriving at an approximate solution to the fundamental vibration mode. Strictly speaking, the seismic response of fill dams involves flexible vibrations in addition to shear vibrations. For this reason, the equation of motion under condition of two dimensional plane strain was earlier solved by the finite difference method. Finite element method (FEM) was developed during the 1950's and used for dynamic analysis of fill dams. Since then with the

progress and application of computers, development of dynamic analysis methods for dams has taken flight. [27]

Considerable progress has recently been made on dynamic tests of actual dams and of models of them as well as earthquake observations. This has been possible due to improvement in the efficiency of exciters and shaking tables, diffusions of them and progressive developments in measuring devices and data-processing techniques. [27]

The stress-strain relationship of soil is non-linear. Thus, the dynamic response of a soil structure should be obtained by a step-by-step integration method, incorporating a load history tracing type model. However, it needs a complicated constitutive equation to describe the whole soil behaviour and it requires a lot of computer time. To simplify the dynamic analysis of soil structures, the nonlinear soil behaviour can be replaced by the linear viscoelastic material. According to this technique called equivalent linear analysis (EQL), an approximate nonlinear solution can be obtained by a linear analysis provided the stiffness and damping used in the analysis are compatible with the effective strain amplitude at all points of the system. [39]

Numerical modeling techniques such as the finite element method were first applied to the dynamic analysis of embankment dams by Clough and Chopra (1966). This was followed by major improvements by Gaboussi (1967), Schnabel et al. (1972), Gaboussi and Wilson (1973), Idriss et al. (1974), Martin et al. (1975), Finn et al. (1977), Lee and Finn (1978), White et al. (1979), Zienkiewicz and Shiomi (1984), Finn et al. (1986), Medina et al (1990), Li et al (1992) and so on. The dynamic numerical codes for fill dams, whether EQL or fully linear, may be the total stress codes (pore pressure not considered) or the effective stress codes. The earlier total stress codes were based on the EQL method of analysis developed by Seed and his colleagues in 1972. EQL is essentially an elastic analysis and was developed for approximating non-linear behaviour of soils under cyclic loading. Typical ones of this type are: SHAKE (Schnabel et al 1972), QUAD-4 (Idriss et al 1973), FLUSH (Lysmer et al 1975) etc. SHAKE is a one dimensional wave propagation program used primarily for site response analysis. QUAD-4, FLUSH are two dimensional versions of SHAKE, used for seismic response analysis of dams and embankments. Due to the elastic nature of EQL analysis, these

codes cannot take into account of material yielding and material degradation under cyclic loading and tend to predict stronger response and cannot predict the permanent deformation directly. “Results in terms of acceleration time histories of linear or equivalent linear analyses performed by shear-beam or FEM can be used as the input for the semi-empirical methods, for example Newmark’s procedures, to assess the dam crest settlement (permanent deformation) indirectly”. More accurate and reliable predictions of permanent deformations can be obtained using the elasto-plastic nonlinear code. Typical ones are: DIANA (Kawai, 1985), ANSYS (Swanson, 1992) and FLAC (Cundull, 1993). These codes use the constitutive models from simple hysteric nonlinear model to more complex elastic-kinematic hardening plasticity models. They provide more realistic analysis of embankments under strong shaking. Marcuson et al (1992) and Finn (1993) used these codes for the analysis of fill dams. [20, 2]

## **2.2 On Problem formulation**

The zoned dam is a heterogeneous continuum structure. Its analysis can best be done by the finite element procedures. The formulation for the elastic isotropic plane strain assumption is summarized below.

The various steps involved in the displacement based finite element analysis are:

1. Subdivision of the continuum into finite elements of suitable configuration.
2. Evaluation of element properties
3. Assembly of element properties to obtain the global (structural) stiffness matrix and load vector. The global stiffness matrix  $[K]$  is obtained by directly adding the individual stiffness coefficients in the global stiffness matrix. Similarly, the global load vector for the system is also obtained by adding individual element nodal loads at the appropriate locations in the global vector, the process is called assembly.
4. Solution of resultant linear simultaneous equations for the primary unknowns (displacements) after introducing the boundary conditions.
5. Determination of secondary unknown quantities, such as stresses and strains.

Since integration is involved in calculation of the finite element relationship for situations for which closed form solutions do not exist, numerical integration is resorted to. A Cartesian coordinate system (x - y) is not convenient for this purpose. The relationship is therefore reduced to a natural coordinate system (ξ - η) in which the element of any quadrilateral shape is transformed to a rectangular one with the extremities at ± 1.

For isoparametric elements such as four-noded quadrilateral or a triangle, the geometry of the element and the displacement function are both described by the same interpolation function and for analysis of dams only such elements are commonly used. For a 2D typical finite element 'e' defined by nodes i, j, m etc., the displacement field {f} = [u v]<sup>T</sup> within the element is expressed as,

$$\{f\} = [N] \{d\}_e = [N_1 N_2 N_m \dots] [d_1 d_2 d_m \dots]^T \dots \dots \dots (2.1)$$

For 4-noded quadrilateral element, the shape functions:

$$N_i = \frac{1}{4} (1 + \xi_i) (1 + \eta_i) \dots \dots \dots (2.2)$$

and ξ, η are the natural co-ordinates of any point within the element.

With displacements known, the strain field as well as the stress field can be determined (i.e. ε<sub>x</sub>, ε<sub>y</sub>, γ<sub>xy</sub> and σ<sub>x</sub>, σ<sub>y</sub>, τ<sub>xy</sub>)

$$\{\epsilon\} = [B] \{d\}_e \dots \dots \dots (2.3)$$

[B] is the strain-displacement matrix.

$$\{\sigma\} = [D] \{\epsilon\} \dots \dots \dots (2.4)$$

[D] is the elasticity (stress-strain constitutive) matrix. For elastic isotropic plane strain analysis:

$$[D] = \frac{E}{(1+\nu)(1-2\nu)} \begin{bmatrix} 1-\nu & \nu & 0 \\ \nu & 1-\nu & 0 \\ 0 & 0 & (1-2\nu)/2 \end{bmatrix} \dots \dots \dots (2.5)$$

E = young's modulus; ν = poisson's ratio of the material

To evaluate nodal displacements, the force-displacement equations are solved using the given boundary conditions.

For an element:

$$\{F\}_e = [K]_e \{d\}_e \dots \dots \dots (2.6)$$

The element stiffness matrix,

$$[K]_e = \int_{vol} [B]^T [D] [B] dV \dots \dots \dots (2.7)$$

For the complete structure:

$$\{F\} = [K] \{d\} \dots \dots \dots (2.8)$$

Figure 2.2a and Figure 2.2b show the face definition of quadrilateral and triangular elements adopted by SAP- 2000. Face definition is useful in assigning the surface pressures on the elements.

### 2.3 On material characteristics and constitutive laws

The Phase-I study report of BMP<sup>1</sup>, the final report of Kulekhani Dam Project<sup>10</sup> are reviewed to fix the density based material properties. For elastic properties of the embankment and foundation materials, relevant literatures<sup>27, 30, 19, 15, 10, 57</sup> are surveyed and reviewed to work out the values. The material data thus fixed are given in Chapter 3.

### 2.4 On direct integration time history analysis technique

The uncoupled modal equations of motion for MDOF system could be solved in closed form if the excitations were a simple function but the time-stepping numerical methods are necessary for complex excitations such as earthquake ground motion. [7]

Time-history analysis is a step-by-step analysis of the dynamical response of a structure to a specified loading that may vary with time. The analysis may be linear or non-linear.

The dynamic equilibrium equations to be solved are given by

$$[M] \{\ddot{u}(t)\} + [C] \{\dot{u}(t)\} + [K] \{u(t)\} = \{r(t)\}; \{r(t)\} \text{ being the response vector relative to ground motion. [44]}$$

Wilson- method is one of such solution techniques. This method , developed by E. L. Wilson, is a modification of the conditionally stable linear acceleration method that makes it unconditionally stable. This modification is based on the assumption that the acceleration varies linearly over an extended time step  $t = \beta \cdot \Delta t$ . The accuracy and stability properties of the method depend on the value of the parameter  $\beta$ , which is always greater than 1. If  $\beta = 1$ , this method reverts to the linear acceleration method, which is stable if  $\Delta t < 0.551 T_N$ , where  $T_N$  is the shortest natural period of the system. If  $\beta = 1.37$ , Wilson's method is unconditionally stable, making it suitable for direct solution of the equation of motion;  $\beta = 1.42$  gives optimal accuracy. [7]

In dynamic analysis of structures and foundations, damping plays an important role. However, due to the limitation in our knowledge about damping, the most effective way to treat damping within modal analysis framework is to treat the damping value of a MDOF system as an equivalent Rayleigh damping in the form:

$$[C] = \alpha [M] + \beta [K]$$

in which  $[C]$ ,  $[M]$ ,  $[K]$  are respectively the damping-, mass- and stiffness- matrix of the physical system;  $\alpha$  and  $\beta$  are the predefined constants called Rayleigh damping coefficients.

As such, in most of the practical engineering analysis, the analyst makes the simplifying assumptions in selecting damping ratios (constant for all significant modes). It is a fact that modal mass participation decreases with increase in modes. Based on above, one can infer that, as mass participation decreases with higher modes, the frequency increases and it is indeed an observed phenomenon. With reduction in modal mass for successive modes, critical damping will decrease with increase in mode. Overall damping of a system being a constant (since total mass and stiffness are constant for a system), the damping ratio will increase with increasing modes. To incorporate this reality, one option may be to compute the Rayleigh coefficients using the following basic formulation incorporating range values for the first significant modes: [8]

$$s = \frac{2\zeta_1 \check{S}_1 - 2\zeta_m \check{S}_m}{\check{S}_1^2 - \check{S}_m^2}; r = (2\zeta_1 \check{S}_1 - s \check{S}_1^2)$$



The modal damping ratio for the soil system would typically be much higher than other civil engineering structures, say 15 to 20 % .[7]

## **2.5 On finite element analysis specific researches on fill dams**

Clough and Woodward, 1967, [48] used the finite element method to analyze a 30.5 m high homogenous dam to study the effect of foundation elasticity and incremental construction on the stresses and deformations in the dam.

Constant values of  $E$  and  $\nu$  were used in the analysis. The results of the gravity turn-on analysis were compared with those obtained from an analysis considering the dam to be built in 10 stages (10 lift increments).

It was found that as far as the stresses were concerned, a single-step analysis gave satisfactory approximation. The horizontal displacements from the two analyses were found to be similar but significant differences were observed in the distribution pattern as well as magnitude of the settlement. While a single-lift analysis, as expected, gave maximum settlement at the top, the incremental analysis showed a small settlement there, while the maximum settlements were observed at about mid-height of the dam.

To study the effect of foundation elasticity on dam behaviour, part of the foundation was also used in the analysis and analyses were performed for different values of foundation elasticity, the lowest being the same as for the dam material and the highest infinite (rigid). It was observed that the vertical stress  $\sigma_z$  was independent of the foundation elasticity, while the horizontal normal stress  $\sigma_x$  and the shear stress  $\tau_{xy}$  varied significantly with it. In general, the stresses reduced as the foundation became softer. The displacement in the dam, however, was very sensitive to the foundation elasticity.

Alberro, 1972, [48] used the finite element method to analyse the 148 m high Infiernillo dam (Mexico), one of the first earth and rockfill structures to be adequately instrumented and thus provided a good opportunity for the comparison of measured values with those calculated by the finite element method.

The dam was idealized into 486 triangular elements and 271 nodes. The foundation of the dam was considered as perfectly rigid.

The non-linear material behaviours were grouped into clay of the core, filters and transitions, compacted rockfill and the loose rockfill. For granular materials, drained triaxial tests and for clay, consolidated undrained tests were taken as representative. Since laboratory data regarding loose rockfill was not available it was assumed that the Young's tangent modulus,  $E_t$ , followed the hyperbolic stress-strain law formulated by R.L.Konder (1963). For core, filter and compacted rockfill, introduction of the values of  $E_t$  in the form of tables was preferred. Relationships for the Poisson's ratio were fixed according to the experimental values of radial strain for filters and rockfill. Due to lack of experimental data for clay, a constant value for  $\nu = 0.45$  was assumed.

The dam was taken as constructed in 7 layers and 3 cycles of iteration were carried out for each stage to arrive at a satisfactory agreement between the Young modulus and the resultant stress condition. The configuration of the vertical deformations along a vertical located at the axis of the clay core, calculated for two successive stages of construction (110 m and 133 m) were plotted and found that at the 110 m stage, the measured and calculated deformations were similar. However, when the dam was raised to EL.133 m, the calculated deformations at EL.95 m differed considerably from those measured. The discrepancy could be attributed to strain hardening behaviour of the soil near the failure zone, which developed in the core as the dam was raised to EL. 133 m. The configuration of the vertical deformation calculated for the same successive stages and along a vertical located in the compacted rockfill downstream of the core showed that the deformations calculated for both stages of construction were excessive and therefore the assumed rigidity of the compacted rockfill was lower than the real rigidity. The analysis was repeated with all assumed values of moduli multiplied by 1.5 and still the comparison between calculated and measured deformations was poor.

The calculated stresses at the end of construction showed the core to be in a state of failure up to EL. 146 m. This was confirmed by laboratory tests undertaken on samples extracted

from the dam core. It was revealed that the material above EL. 145 m had undergone a process of consolidation subsequent to construction under stress conditions such that the principal stress ratio was relatively low, which resulted in gain of strength. However, the material in the core below EL. 145 m was revealed to have lost strength and to have absorbed water. In this case the material had evolved under a stress condition where  $\sigma_1/\sigma_3$  ratio was high. An important conclusion of this study was that results of analysis were sensitive to deformability parameters as the deformation moduli of materials computed in the field differed from those in the laboratory. Field compaction induced what were, in effect, confining pressure, which acted similar to preconsolidation stresses.

Knight and colleagues, 1985, [48] used the concept of back analysis by the finite element method to study and interpret instrumentation readings taken during the construction, impounding and full reservoir stages of the life of Mona Savu dam in Fiji, the 85 m high embankment with rockfill shells supporting a wet, halloysitic residual clay core, situated at Mona Savu Falls. It has a central core of modest width inclined slightly off vertical. Analysis involved adjusting the elastic deformation parameters of a simple well-established model of material behaviour to ensure the best correspondence between computed and observed behaviour.

A linear elastic finite element program was used for the analysis. The program could analyze two-phase elastic media consisting of an elastic skeleton with pore fluid. The analysis employed known pore-pressure change analysis at each stage of construction and impounding. The mesh consisted of 8-noded isoparametric elements. The bedrock was assumed to be rigid. The filter and transition zones were assigned the same elastic parameters as the rockfill shells. Embankment construction was modeled by five fill layers and impounding was modeled in three stages. The final stage of construction overlapped with the first stage of impounding.

The back analysis was carried out on a trial-and-error basis and sets of isotropic elastic deformation parameters were found for the core and shells which satisfactorily reproduced the measured behaviour for all the modeled stages. The rockfill was assigned a single pair of elastic parameters for all stages of analysis. For the core a constant value of the Poisson's

ratio of 0.4 was taken while the value of E was varied with effective vertical stress (constant value up to  $1.50 \text{ kN/m}^2$  and thereafter linearly varying with  $z$ )

Good agreement was observed between the measured and computed settlements. The model slightly underestimated the support given to the core by the downstream shell but during impounding differences appeared; in the model much of the core showed upward movement whereas the measured core movements, although decreasing, were still downward. These differences were considered to be due to settlement in the upstream shell in the prototype caused by saturation, which more than compensated the uplift due to buoyancy. The computed stresses in the core also agreed satisfactorily with the measured values.

Panos Dakoulas and George Gazetas, 1986, [11] made an investigation on the seismic shear strains and seismic coefficients in dams and embankments. A comprehensive comparative study was undertaken using five dam cross-sections, each excited by four recorded accelerograms. Particular emphasis was given in studying the effects of material inhomogeneity which chiefly depends on the variation of the shear modulus with confining pressure, the size and relative stiffness of the core, as well as the geometry of the dam or embankment. It was shown that the average shear modulus  $G$  across the width of a dam may be expressed as a power  $m$  of the  $z$  coordinate:  $G = G_b \left(\frac{z}{H}\right)^m$ ; in which  $\frac{z}{H}$  is the relative height and  $G_b$  is the average shear modulus at the base ( $z = H$ ). It was mentioned in the paper that the value of  $m$ , which encompasses the effects of the aforementioned inhomogeneity factors, usually varies from 0.40 to 0.75; the lower values of  $m$  in this range are typical for steep rockfill dams consisting of compacted coarse gravel, whereas the higher values are representative of earthfill dams having a soft and wide cohesive core and silty-sandy shells. It was found that plane-strain finite-element analyses yield distributions of peak values of seismic shear strains which, in general, are in good accord with the results of a consistent inhomogeneous SB model.

Sara J. Lacy and Jean H. Prevost, 1987, [31] proposed a general and efficient numerical procedure for analyzing the dynamic response of geotechnical structures, which are considered as both nonlinear and two phase systems; and made the elasto-plastic earthquake

response analysis of a two phase nonhomogeneous earth dam; Santa Felicia dam to the San Fernando earthquake, using the developed numerical procedure.

The two dimensional finite element model-meshes, representing the maximum cross section of the dam, consisted of 156 nodes. Each node was assigned 4 possible degrees of freedom; two perpendicular directions of soil displacement and two perpendicular directions of fluid velocity. For purposes of the analysis, the reservoir was assumed at the maximum water level. The phreatic line was located by the conventional standard procedure which divided the dam into 66 saturated elements and 67 dry elements with nodes having no fluid degrees of freedom. The results of the numerical calculations were compared to the extensively recorded response of the dam. It was found that the calculated response compared well with the recorded response of the dam at the crest during an earthquake.

N. Uddin, 1997, [52] devised a single step procedure for estimating seismically-induced displacements in embankment dams. Estimation of the permanent deformations of embankment dams by sliding block analysis is based upon the simplifying assumption that dynamic acceleration response and wedge sliding are two separate processes (decoupled “elastic” and “rigid slip” features of the dynamic response). An alternative hypothesis was proposed in this paper, namely that these two processes occur simultaneously. To this end, the dam was assumed to contain a priori assigned, potentially-sliding interface, and the dynamic response was computed in a single step. As a validation of the new single-step procedure, a numerical analysis was carried out and shown to successfully explain the asymmetric response of La Villita Dam recorded during the Mexico earthquake of 15 September 1985. All analyses were performed with ADINA using special interface elements to model the slip and Newmark’s time integration algorithm for a direct step-by-step solution.

V. Mircevska and V. Bickovski, 1998, [36] performed the two dimensional nonlinear dynamic analysis of rockfill dam. Investigations were performed by consideration of effective stresses wherefore the distribution of pore pressure through the coherent media was analyzed previously. The differential equation of motion was solved by using the incremental

step-by-step linear acceleration method which incorporated the Wilson- method for direct integration. The prepared software package PROCESS was applied for a rockfill dam with a height of 85 m excited by the Imperial Valley earthquake with  $a_{\max} = 0.36g$ . Within each time increment conducted was the iterative procedure referred to as “Load Transfer Method” which enables balancing of the residual forces and satisfying of the dynamic equilibrium conditions within the considered time increment. A comparison between the obtained nonlinear dynamic response and the linear response of the system was made. The stability of the structure was checked by both linear and nonlinear treatment.

Jafarzadeh and Alireza Yaghubi, 1998, [24] evaluated the effect of narrow canyons on the dynamic response of zoned rockfill dam by performing the plane strain analysis as well as 3-D analysis. The effect was evaluated on natural frequencies of an embankment dam by FEM method. Canyon geometry of a real zoned rockfill dam under construction and some other typical canyon geometries like rectangular, trapezoidal and triangular shapes were considered. The first ten natural frequencies and their corresponding mode shapes were calculated for each case and compared with each other, to evaluate the stiffness effect of the abutments on natural frequencies. Concerning the results of this paper, it was concluded that at dam sites with length to height ratio (L/H) less than 4, the three dimensional behaviour affects the dynamic responses and that it could not be neglected in seismic design of embankment dams.

Ernesto Cascone and Sebastiano Rampello, 2003, [5] evaluated the seismic stability of an earth dam via the decoupled displacement analysis using the accelerograms obtained by ground response analysis to compute the earthquake-induced displacements. The response analysis of the dam was carried out under both 1D and 2D conditions, incorporating the nonlinear soil behaviour through the equivalent linear method. Ten artificial and five real accelerograms were used as input motions and four different depths were assumed for the bedrock.

1D and 2D response analyses were in a fair agreement with the exception for the top third of the dam where only a 2D modeling of the problem could ensure that the acceleration field is

properly described. The acceleration amplification ratio obtained in the 2D analyses was equal to about 2 in all the cases considered, consistently with the data from real case histories.

The maximum permanent displacements computed by the sliding block analysis were small, being less than 10% of the service freeboard; a satisfactory performance of the dam could then be envisaged for any of the seismic scenarios considered in the analysis.

## **2.6 On seismic design guidelines/codes for fill dams**

“IITK-GSDMA Guidelines for Seismic Design of Earth Dams and Embankments” [22] is the only reference code accessible during the present research work. It recommends the hydrodynamic loads to compute via Zangar’s formulation (Art. 9) and for this; formula and charts are given. It also contains the chart to compute the permanent displacements by sliding block analysis (Art. 7) based on the Newmark’s slope stability analysis procedures.

## **3. NUMERICAL MODELING**

### **3.1 General**

The zoned rockfill dam of the proposed BMP, Nepal; having more acquainted with and having relatively more information available, is chosen as a typical case for the numerical modeling. SAP2000 (V10.0.1) software package is used as the numerical tool. Plane strain assumption is used for the 2-D finite element analysis.

### **3.2 Problem geometry / Finite element mesh**

#### **3.2.1 Embankment section**

BMP high dam is a zoned type rockfill dam with central earth (clay) core. Figure 3.1 shows the maximum cross section of the dam designed as per the classical empirical methods. The dam is 117 m high above the lowest foundation. The crest is 10 m wide and about 700 m long. So the ratio of length between canyon walls and height of the maximum cross section, L/H is about 6.

#### **3.2.2 Finite element model**

The 2-D plane strain assumption is made based on the rationale that the L/H ratio is greater than 5 [5, 24]. The finite element mesh consists of Isoparametric quadrilateral and triangular elements. To simulate the lift construction and incorporate the inhomogeneity<sup>11</sup>; with the assumption that core is more affected [Knight and colleagues, 1985], the core is divided into ten different layers. Two models are adopted; one with rigid foundation (all nodes at the base fully restrained) and other incorporating foundation flexibility by taking some part of foundation. The boundary conditions for this model are such that all the bottom nodes are restrained in all directions while vertical nodes at either side of foundation are restrained against translation in horizontal direction in addition to the common plane strain restraints.



Regarding the effective part of foundation to be taken in the model, the first issue that this research is expected to address, the stress criterion aforementioned in section 1.3 is used. For this, a number of trials with increasing dimensions of foundation on either side and underneath the embankment is made until the stresses at the boundaries comes out with negligible vertical stress (minimum stress taken around 10 to 20 percent of the maximum stress at the contact point below the core of main dam). The foundation beyond this effective part is neglected. The final size worked out initially with approximate material properties is such that it was twice the base width of embankment section on either side and four times of the base width underneath the embankment. This model, when checked after all properties are finalized reveals that the minimum stresses at the extreme boundaries of the model is only around 5% of the maximum stress just below the embankment at the centre. A distribution of foundation pressure bulbs (vertical stress contours) during the trial procedure is given in figure 3.2.

Figure 3.3 and figure 3.4 respectively show the two dimensional finite element models thus worked out; former with rigid foundation (RF model) and the later with flexibility of foundation considered (FF model).

For the purposes of analysis, the reservoir is assumed at the maximum water level (TWL). The corresponding free surface of water (phreatic line) in the core is located using the procedure described in reference 37 and is summarized in appendix D. Computation of the point of the corrected line on the downstream discharge face of the core is followed by the approximate layout within the core by eye judgment. Calculation results the aforesaid point on downstream discharge face to locate at a height around 0.55 times the height of the core above its base level. Below this phreatic line, the elements are saturated and elements above this line are assumed dry (unsaturated). The FF\_WR model demonstrating the division of core into saturated and dry parts is presented in Figure 3.5. A summary of calculation for phreatic line is included in appendix D.

### 3.3 Material properties

BMP high dam consists of impervious clay core covered by rock, gravel and random fill shells resting on a stiff foundation layer of gravel and sand alluvium deposit down to bedrock. The rock types available nearby are reported to consist mainly of shale and sandstone [1]. The clay is assumed to be of rolled stiff type. Based on this general information available in the report<sup>1</sup>, literatures mentioned in section 2.3 are surveyed and the material characteristics are assumed. In fact, confidence on the reliability of these would only be achieved if the arrangements for the tests that can more simulate the in-situ situation could be made, which is supposed to be beyond the scope of present thesis.

Table 3.1 presents the information regarding the densities of homogeneous materials under normal condition and under saturated condition. The shells are assumed free-draining, the core to have very low permeability and the rock foundation to be fully impervious.

Regarding the elastic properties (modulus of elasticity and Poisson's ratio) required for the linear elastic analysis, the materials are assumed to be homogeneous, elastic and isotropic except for core which, as already mentioned before, is divided into ten different layers but each layer again following the above assumptions. Due to the lack of experimental data, all the shells and filter are assigned the same elastic parameters. The elastic material data used in this investigation are assumed to be the drained triaxial test results in the case of shells and the undrained triaxial test results for the case of core; and at the end-of-construction stage. These data for the unsaturated materials are presented in table 3.2. For saturated materials, again due to the lack of data, an assumption is made. Due to the assumption that the rock skeleton are intact and shell body is free draining, the elastic parameters are not likely to change appreciably; the only effect could be the very small contribution made by water as lubricant. However, due to the effect of water, the clay minerals are likely to react and the core material may suffer degradation of strength. To incorporate this effect and also the enhanced pore pressure which ultimately reduce the strength, the elastic modulus of the clay is assumed to reduce by 15 %. [19, 27]

### 3.4 Input ground motion

Due to the lack of records of any strong earthquake ground motion in the vicinity of the BMP dam site, the famous imperial valley earthquake of May 18, 1940 (El Centro, California, USA) [USGS ] is chosen. Both the N-S and vertical components are used. Figure 3.6 shows the input ground acceleration time histories of the excitations in the upstream-downstream (N-S component) and vertical directions (vertical component) of the dam.

### 3.5 Modeling of water pressures

In the case of a region with high permeability such as a rock zone, it may be safely assumed that no steady state infiltration force is developed. When the rate of change in level of stored water is high, so that the impervious zone is not in a steady state infiltration condition, an unsteady seepage force develops. But since it is extremely complicated to consider the unsteady seepage force in dynamic analysis, the situation is sometimes simplified by assuming that the static hydraulic force acts on the upstream side of the impervious zone.

[27]

The present investigation follows this basic idea.

The hydrostatic pressure at any depth  $d$  below the free surface of water is given by  $\gamma_w \cdot d$  normal to the surface;  $\gamma_w$  being the unit weight of water. Thus if the height of water surface above the base on the core is  $H$ , then the static water pressure at a height  $z$  above the base is given by  $\gamma_w (H-z)$ . This linear pressure distribution of water pressure can be assigned to the nodes on the u/s face as the area surface pressure loads by assigning joint pattern. The joint pattern available in SAP-2000 is in the form  $A x + B y + C z + D$ ; so for  $z$  measured above the bottom of core,  $A = 0$ ,  $B = 0$ ,  $C = -1$  and  $D = H$  and the multiplier for surface pressure load =  $\gamma_w = 9.81 \text{ kN/m}^3$ .

Regarding the hydrodynamic pressures induced due to earthquake vibration, IS recommendation is simply followed in the present research. Hence hydrodynamic added pressures are computed based on Zangar's formulation [22]. The pressures are converted into nodal forces on the basis of tributary area simply by integrating the definite integral of

regression curve representing the hydrodynamic pressures, for the case of pseudo-static analysis. For the case of time history analysis, equivalent virtual added masses are lumped on the upstream nodes of the core. Not considering the reservoir-embankment interaction is reported<sup>20</sup> to have negligible effects when the natural frequency of the reservoir is larger compared to that of the dam system and fortunately the present system satisfies this criterion. The hydrodynamic pressure forces are equated to the equivalent inertial forces added by the reservoir and hence the shape of the body of reservoir that can be assumed to move with the dam system is worked out. Again, the added masses to be lumped as the nodal masses are computed on the basis of tributary areas. Table 3.3 and 3.4 show the calculated equivalent static hydrodynamic loads and the equivalent hydrodynamic added masses for the main dam core and the core of the upstream coffer dam, over which the main dam is constructed. A summary of calculation is incorporated in appendix C.

## 4. NUMERICAL ANALYSIS

### 4.1 General

All calculations are performed on a PC using the software package SAP2000 (V10.0.1). Dynamic analysis of the models worked out earlier in chapter 3 to the prescribed earthquake ground motion is the key objective in this research.

Narrowly speaking, dynamic analysis refers to the response analysis carried out to determine stress or deformation, considering only the earthquake force. The ultimate objective in carrying out dynamic analysis of a fill dam is to evaluate dam safety against sliding or liquefaction based on the calculated values of stress and deformation. In the case of fill dam, however the static initial stress conditions considerably affect the stress developed during an earthquake as well as the ultimate stability. Efforts are ongoing to accurately estimate the behaviour of fill dams during earthquakes based on the development of finite element methods and true representation of the nonlinear constitutive relationship of the soil subjected to cyclic (repetitive) loads, in order to precisely estimate the behaviour of a fill dam during an earthquake. This trend is on the rise. [27]

In present investigation, first, the free vibration analysis and initial static deformation analysis have been carried out with the purpose of getting acquaintance and confidence with the models worked out in chapter 3. The first and the last mode natural periods for the first twelve significant modes are also used to compute the Rayleigh damping coefficients in direct integration time history analysis. Then for the stability check, as aforesaid, simplified decoupled technique is adopted. For this, linear time history analysis is performed which is then followed by the calculations for the permanent deformation using the chart developed based on Newmark's stability analysis procedures. .

### 4.2 Free vibration analysis

In order to obtain the natural frequencies and mode shapes, the global mass matrix and the global stiffness matrix need to be computed to solve the eigen value problem. The eigen

values yield natural frequencies and the eigen vectors corresponding to the eigen values give the mode shapes. This job is carried out in present work by the inbuilt modal analysis facility available in SAP2000. The first twelve modes, by default in the program, are considered as they contributed to more than 99% of modal mass participation. It is observed that taking five modes, as generally done for framed building structures, contributes even not more than 90 % in mass participation. Table 4.1 shows the natural periods of the first twelve significant modes of the RF and FF models of the BMP and Figure 4.1 shows the first twelve significant mode shapes with the FF model, for example. In both models, it is found that the modes are basically constituted by core deformations.

### **4.3 Initial static analysis**

In the whole of this thesis, the response in terms of deformations, basically settlement is the major concern as discussed on section 1.2. The linear static analysis at the end-of-construction stage is performed. Investigation on the deformations within the core is focused as they may be relatively of more interest. Figure 4.2a and figure 4.2b show the distribution of vertical displacements (settlement) along a vertical through the core-centre and along a horizontal through maximum settlement. The associated data are shown in table 4.2 and table 4.3.

### **4.4 Time history analysis**

The linear time history analysis is performed for both RF and FF models excited by El Centro earthquake ground motion the prescribed earthquake as mentioned in section 3.4, The step-by-step direct integration method based on Wilson- incremental algorithm which is inbuilt in SAP-2000 is used with  $\beta = 1.42$  as mentioned in section 2.4. Rayleigh damping coefficients are computed based on the reference formulation given in the same section. The damping variation, as prevails for the geotechnical system, is taken between 10 to 20 % corresponding to the first and the twelfth significant modes considered. The damping coefficients thus computed are presented in table 4.4.

Each RF and FF model is analyzed for two cases: one without reservoir (WOR) and other with reservoir (WR); so, in total, four sets of results are obtained namely for RF\_WOR, FF\_WOR, RF\_WR, and FF\_WR. For WR models the virtual hydrodynamic added masses are computed as detailed in section 3.5 and appendix C, and lumped at the u/s face of the core of the main dam and both u/s and d/s faces of the core of the coffer dam. The computed time histories of the peak acceleration at the crest of the dam for these four cases are shown in figure 4.3a, figure 4.3b, figure 4.3c and figure 4.3d respectively.

## 5. INTERPRETATION AND VERIFICATION OF RESULTS

### 5.1 General

The critical study of the results of numerical analysis reveals some important findings. Various parametric investigations are made to verify the results. The discussions on the results are presented separately under sections 5.2 through 5.5.

### 5.2 Effective foundation geometry

As mentioned in section 3.1, the geometry of the effective foundation to be considered for FF model comes out to be twice the base width of the dam on either side and four times the base width on the underneath. The pattern of the vertical stress contours compares well with the pressure bulbs obtained by the classical theory of soil mechanics [37, 12, 32].

To verify the magnitudes as well, a simple finite element plane strain model of a long concrete wall (1 m thick, 3 m height;  $E = 2 \times 10^4$  MPa,  $\nu = 0.20$ ) founded on a clayey soil ( $E = 20$  MPa,  $\nu = 0.42$ ) is prepared in the same way as done for BMP dam using the same SAP 2000 software package. The vertical stress contours thus obtained under the gravity load of the wall are shown in figure 5.1. This problem is taken as the line load case of classical soil mechanics and the vertical soil stresses at different locations in the foundation are computed and found comparable with those obtained by the FE analysis. As an example, at a depth of 2 m vertically below the centre, FE solution gives a vertical compression stress equal to 21.81 KN/m<sup>2</sup> while the soil mechanics formula for line load case [37] for this point gave

$$\tau_z = \frac{q}{z} \frac{2}{\pi} = 22.92 \text{ KN/m}^2; \text{ since } z = 2 \text{ m and } q = (1 \times 3) \times 24 = 72 \text{ KN/m.}$$

Thus the stress computed by FEM differs from that calculated based on classical soil mechanics by only around 5 %.

Also the parametric studies are made which reveals the negligible effects of the elastic parameters on the vertical foundation stresses complying with the soil mechanics formula



and also with a finding of a previous research by Clough and Woodward (1967) reviewed in chapter 2.

Thus, the foundation stresses predicted by the so worked out FE model are justified and the effective geometry derived based on the stress criterion may be taken as a reliable result. Thus the very first objective is achieved.

For the practical use, these dimensions may be little bit reduced to allow more stresses; around 20 % as recommended by Terzaghi [37], to reduce the degrees of freedom and hence the computational time

### **5.3 Free vibration periods**

The fundamental natural periods of vibration for the models considered in this research are calculated to be 0.87729 sec for the RF model and 1.19573 sec for the FF model.

The study on fill dams in Japan [27] suggests the formula to estimate the fundamental vibration period of fill dams as a function of height, as:

$$T = 0.01 H \quad \text{for earthfill dams}$$

$$T = 0.005 H \quad \text{for rockfill dams}$$

According to this formula, the fundamental natural period of BMP dam, 117 m high above the lowest foundation level, should come at most 0.585 sec; which shows large discrepancy. Though the natural period cannot simply be taken as the function of height of the structures solely, it is surprising why such formulation is recommended or why the present model under investigation doesn't satisfy that; question arises whether the model that gives satisfactory foundation stresses under static gravity loading condition is not working for the vibration analysis.

To gain confidence with the results, parametric studies are made taking a number of models of different proportions; all symmetrical about the central vertical axis and the foundation base at the same level. It is found that the models of the fill dams designed based on some standard specification [30]; for example crest width around 10 m and base width about 4.5 times the height, material density near 21 kN/m<sup>3</sup>, exactly satisfies the above mentioned

formula provided the dams are homogeneous with the elastic parameter values  $E = 2000$  MPa,  $\nu = 0.38$  for rockfill dam and  $E = 500$  MPa,  $\nu = 0.40$  for earthfill dam. This is really an important innovative parametric study carried out in this thesis. The finite element model (2-D model, plane strain assumption, finite element meshing) and the modal analysis procedure adopted in the present research, via SAP2000 as a tool, can therefore be concluded to be valid.

It is interesting to observe that the same symmetrical homogeneous dam which exactly satisfies the above relation comes out with a drastic change in the value of the fundamental natural period after a soft central clay core is introduced. For example, a homogeneous rockfill dam of height 57 m (equivalent to the upstream coffer dam of BMP dam) satisfying the aforesaid specification gives the natural period of 0.28 sec; almost equal to  $0.005 H$ . The same dam gives the natural period of 0.23 sec if only the young's modulus is changed from 2000 MPa to 3000 MPa, and gives the natural period of 0.78 sec when a clay core ( $E = 20$  MPa,  $\nu = 0.42$ ) is introduced to convert it into the zoned rockfill type; the discrepancy of around 179 % from the original value. Figure 5.2 and figure 5.3 show the first twelve significant modes of the model rockfill dam without core (homogeneous) and with core (zoned) respectively.

The zoned rockfill dam model of BMP worked out in the present research has complex geometry and combination of different classes of materials; and is unique in itself. Therefore, getting some unique value of natural period for this particular case, with the valid finite element model and analysis procedure, is taken justifiable.

Also from the basic principle that as the stiffness of a structural system is reduced, the natural period increases, the zoned rockfill dam, with the core having density comparable while young's modulus very small relative to the shell, must have natural period very high compared to the homogeneous rockfill dam. The same principle also justifies the increased natural period of FF model with respect to RF model.

## 5.4 Initial static deformations

The vertical displacement (settlement) profile within the core for the linear static analysis under the self weight load at the end-of-construction stage shows an increasing trend from base towards crest until some depth below the crest where maximum settlement occurs and again decreases for the portion over it.

This is different from the general perception that the maximum elastic settlement of an embankment under its self weight is at the crest. The finite element investigation of a homogeneous fill dam carried out by Clough and Woodward, 1967, reviewed in chapter 2, also found the similar result for the gravity turn-on analysis. Therefore, it is again required to verify that the BMP dam model of the present research can work for the embankment deformation analysis as well, in addition to the analysis for foundation stresses and free vibration analysis.

Parametric studies are performed taking a small symmetrical rockfill dam model (equivalent to the upstream coffer dam of the BMP dam). First, this zoned rockfill dam is analyzed and the settlement profile are captured. Second, the dam is assigned with homogeneous material properties, analyzed and again the settlement profile is captured. The studies suggest, as generally expected, that for the homogeneous fill dam, under gravity loads without reservoir, the settlement increases from base toward crest; with steep increase at the bottom portion while difference is small toward crest. This again validates the adopted finite element model. Investigations with varying material properties too lead to the same trend. Figure 5.4 presents such profile, for instance. But, the introduction of core in zoned rockfill dam gives the same trend as obtained in the present research on BMP dam. Figure 5.5 presents such profile. It is interesting that the even the present unsymmetrical BMP dam model follows the former trend when assigned with homogeneous material properties. For the purposes of analysis, the core of the zoned dam when assigned with some hypothetical material stiffer than the shell also exhibits similar trend with maximum settlement at the crest.

Thus it is justified that, it is the relative stiffness of the weak core and strong shell of a zoned rockfill dam that results the profile of settlement in the core as obtained in the present

research. One more possibility, beyond the scope of this research due to different limitations, may be to investigate the effect of modeling the slippage at the core-shell interface of a zoned dam as likely to occur in reality. This is discovered as a potential sophisticated investigation for future as defined in chapter 7.

## **5.5 Time history results and permanent settlements**

The peak horizontal crest accelerations of the history as obtained from the time history analysis are presented in table 5.1.

The permanent settlement in the present research is obtained by the indirect semi-empirical method (decoupled approach) based on Newmark's analysis procedures (NAP).

As per the chart developed based on the NAP, the permanent crest settlement of the crest of a fill dam is obtained as a function of the ratio of yield acceleration to the peak crest acceleration during earthquake excitation.

This displacement thus obtained is assumed to be the crest settlement [2].

The yield acceleration is defined as the average acceleration producing a horizontal inertia force on a potential sliding mass so as to produce a factor of safety of unity thus causes it to experience permanent displacement. The yield acceleration is essentially the horizontal seismic coefficient which gives the limit equilibrium factor of safety of unity when based in a conventional slope stability analysis. This value is assumed to be 0.15 g in the present research; simply based on the suggestion by Seed (1979)<sup>20</sup> that a seismic coefficient of 0.1g for magnitude 6.5 earthquakes and 0.15g for magnitude 8.25 earthquakes may be taken to obtain a factor of safety of 1.15.

Knowing the yield acceleration and the peak crest response acceleration from time history analysis, the permanent settlement of the embankment is calculated using the upper bound relationship (8.25 magnitude earthquakes) of the chart given in IS guidelines<sup>22</sup> suggested by Hynes-Griffith and Franklin (1987). The chart is reproduced in figure 5.6. Table 5.2 presents the results. It is found that the RF model is more conservative for seismic safety analysis. The results also show that the permanent settlement for the BMP dam evaluated by four different

models are relatively higher; nonetheless they are within the acceptable limit of 1 m stipulated in the reference guideline except for one model (RF\_WR), the model which is conservative in itself.

## 6. CONCLUSIONS

### 6.1 Answers to the research questions

The present research is to address the two major issues as detailed in section 1.2. First, what should be the geometry of the effective part of the foundation to be taken in the numerical model of a given zoned rockfill dam? Second, what would be the dynamic response of a zoned rockfill dam that was designed by traditional empirical methods, when excited by the prescribed earthquake ground motion? The whole of the effort is expended in this research to address these two issues though a number of parametric studies are made to gain confidence with the finite element models exercised. A summary of answers to these two major research questions is given below.

1. To deal with the BMP zoned rockfill dam having irregular geometry and complex distribution of material, FEM is used. A vertical stress criterion under the self weight load of the dam is used to investigate the effective geometry of the foundation. The effective geometry of foundation for the considered BMP dam; obtained by trial procedures based on the stress criterion, comes out to be twice the base width on either side and four times the base width underneath the dam. Analysis of the dam model with this geometry of foundation considered gives the minimum pressures in foundation boundaries equal to around 5 % of the maximum contact pressure, after all material properties are finalized.

2. The stability analysis of the BMP zoned rockfill dam, which was designed based on traditional empirical methods, is carried out based on the decoupled finite element deformation analysis technique. Four different models, RF and FF models, each with and without reservoir are evaluated. The linear direct integration time history analysis (dynamic analysis) of the derived finite element models of the BMP dam under the ground motions due to the El Centro earthquake as the prescribed one are carried out to evaluate the peak crest acceleration which is then followed by the permanent settlement analysis based on Newmark's analysis procedures in reference to the IS guideline. The permanent settlements come out relatively higher; nonetheless they are within the acceptable limit of 1 m stipulated in the reference guideline except for one model (RF\_WR), the model which is conservative

in itself. So, still higher value of the freeboard than the proposed may be provided in the final design and construction of the BMP high dam since the risks associated with such a large and very important structure are high.

## 6.2 List of general findings

1. The first twelve modes, default in SAP2000, for the BMP zoned rockfill dam are found to contribute more than 99% in mass participation. Taking first five modes are found to contribute even not more than 90 % in mass participation. Therefore the first twelve modes are considered as the significant modes for further calculations.
2. The first and the twelfth vibration periods (in seconds) for the RF\_WOR and FF\_WOR models are found to be 0.8773, 0.4244 and 1.1957, 0.4981 respectively. The periods for FF model are higher than that for RF model.
3. The JSCE recommendation to estimate the fundamental natural period of rockfill dam from  $T = 0.005 H$  is found to be satisfied exactly by the symmetrical homogeneous rockfill dams, that comply with the general specification of geometry proportioning and having elastic parameters  $E = 2000 \text{ MPa}$ ,  $\nu = 0.38$  and density around  $21 \text{ KN/m}^3$ . Similarly, the estimate of fundamental period from  $T = 0.01H$  for earthfill dam is found to be satisfied exactly by the symmetrical homogeneous earthfill dam which comply with the general specification for geometry proportioning and having the elastic parameters:  $E = 500 \text{ MPa}$ ,  $\nu = 0.40$  and density around  $21 \text{ KN/m}^3$ .
4. If a soft core is introduced in the homogeneous rockfill dam to make it zoned, the natural period increases drastically.
5. The initial static settlement profile of the core of a zoned rockfill dam along a vertical due to gravity turn-on load is different from that of the homogeneous rockfill dam. For a homogeneous fill dam, the settlement increases from base toward crest; with steep increase at the bottom portion while difference is small toward crest. But for a zoned rockfill dam, the maximum settlement is not at the crest; it is maximum at some one-third of height below the crest instead.

6. In both homogeneous and zoned cases, however, the settlement variation in horizontal section is such that it is maximum at the centre and decreases on either sides.
7. Under single step gravity turn-on load, the linear elastic analysis reveals that the settlements obtained from RF model are small compared to those from FF model.
8. The maximum hydrodynamic pressures on BMP dam core obtained from Zangar's formulation as recommended in IS guidelines is about 40 % of the maximum static water pressure.
9. For WOR seismic loading, the RF model estimates larger value of permanent settlement; hence RF model for seismic analysis is conservative.
10. Taking foundation elasticity into account in the finite element modeling proves very sensitive to deformation behaviour.

### **6.3 Concluding Remarks**

Using simplified technique of 'decoupled deformation analysis', the seismic safety of a zoned rockfill dam which was designed by the traditional empirical methods, taking BMP high dam as a typical case, is assessed. Although the finite element modeling exercised using SAP2000 as a tool is found to yield results that compare well with the classical soil mechanics and the past studies reviewed, it should be checked with more rigorous nonlinear dynamic analysis incorporating the complex constitutive models. Also, performing the experimental model tests may impart more confidence to arrive at the final state-of-the-art methodology to be adopted for such a very large and important structure in the high seismic zones of Nepal.



## **7. RECOMMENDATIONS FOR FUTURE WORKS**

### **7.1 General**

Many potential research works for future on the zoned rockfill dam are identified during the present thesis. These couldn't be realized in this work due to the limitations of time, knowledge and resources. The recommendations for the future works are summarized under three categories viz. Improvements, Additions and Sophisticated advanced research.

### **7.2 Improvements**

1. Investigation with zoned rockfill dam - specific software packages.
2. Investigations with real tested material properties of the site.
3. The assessment of the design ground motion at the dam site, including reservoir triggered seismicity (RTS).
4. Modeling of discontinuities at the interfaces such as shell-filter-core and dam-foundation.
5. Detail investigations on reservoir-dam interaction.
6. Parametric investigations with different dam geometries and different material properties.
7. Investigations with 3D Finite Element Modeling.
8. Rigorous non-linear dynamic investigations incorporating the path and time dependent constitutive models.

### **7.3 Additions**

1. Investigations with modeling for the pore pressure incorporation.
2. Investigations incorporating draw down seepage forces and cavitation effects.
3. Investigations with different types of foundation soils including seismic liquefaction.
4. Investigations for stage (incremental/multiple lift) construction and effect of reservoir filling.

5. Numerical investigations on effectiveness of preventive and remedial measures stipulated in design guidelines.

#### **7.4 Sophisticated advanced research**

Experimental model investigation using shaking table test, for instance, may be carried out to quantify the interactions at the core-shell interfaces. Then the research shall be focused to devise, from the first principle, the interface elements and formulate the appropriate constitutive laws so that nonlinear dynamic analysis simulating the real behaviour of the zoned rockfill dam may be carried out. An example of such formulation for an arch dam is given in reference 48. Similar investigations may be performed to simulate the grain-to-grain contact nonlinearity among the shell skeletons by micro- modeling.

## REFERENCES

1. “Bagmati Multipurpose Project, Phase-I Feasibility Report, Annex 18: Bagmati High Dam and Hydroelectric Development”. NEA-library, Nepal, 1980
2. Baldovin, E., Paoliani, P. “Dynamic analysis of embankment dams”
3. Bathe, K. J. and Wilson, E. L. “Numerical Methods in Finite Element Analysis”. Prentice Hall, NJ, 1967
4. Bhookya, M. “Analysis of earth and rockfill dams during earthquakes”. M. Tech. thesis, Department of Civil Engineering, IIT-K, India, July 2001
5. Cascone, E., Rampello, S. “Decoupled Seismic Analysis of an Earth Dam”. Soil Dynamics and Earthquake Engineering, 2003, 23, 349-365 \*
6. Chakrabarti, P., Chopra, A. K. “Earthquake Response of Gravity Dams Including Reservoir Interaction Effects”. Report no. EERC 72-6, Earthquake Engineering Research Center, University of California, Berkeley, California, 1972
7. Chopra, A. K. “Dynamics of Structures”. Pearson Prentice Hall, India, 2005
8. Chowdhary, I. , Dasgupta, S. P. “Computation of Rayleigh damping coefficients for large systems”
9. Clough, R. W., Penzien, J. “Dynamics of Structures”. McGraw Hill, Inc, 1993
10. Consulting Engineers, Nippon Koei Co. Ltd., Tokyo. “Kulekhani Hydroelectric Project, Project Completion Report”. HMG of Nepal, Kulekhani Hydroelectric Development Board, 1983
11. Dakoulas, P., Gazetas, G. “Seismic shear strains and seismic coefficients in dams and embankments”. Soil Dynamics and Earthquake Engineering, 1986, 5(2), 75-83
12. Das, B. M. “Principles of Geotechnical Engineering”. Thomson Books/ Cole, 2004
13. Dhakal, S. et al. “Analysis and Design of Storage Type Hydro-Project (BMP)”. B.E. Project Report, Dept of Civil Engineering, Pulchowk Campus, IOE, TU, Nepal, 2005
14. “Earthquake Analysis Procedures for Dams, state of the art”. Bulletin 52, CIGB, ICOLD, 1986
15. “Final Report of Soil Investigation Work for Proposed Lalitpur Bishalbazar Commercial Complex”. CMTL, Department of Civil Engineering, Pulchowk Campus, IOE, TU, Nepal, 2002

16. "Final Report on Feasibility Study Level Analysis (Updating Parameters) of Bagmati Multipurpose Project". Report submitted to WECS, HMG/N by Hydro-Engineering Services (P) Ltd., July 1999
17. Gaur, V. K. "Earthquake Hazard and Large Dams in the Himalaya". Proc. of the INTACH workshop in reference to Tehri Dam, Jan 15-16, 1993
18. Gautam, N. S. "Response of Barrages to earthquake ground motion including hydrodynamic effects". M. Sc. Thesis, Department of Civil Engineering, Pulchowk Campus, IOE, Pulchowk Campus., 1999
19. Goodman, R.E. "Introduction to Rock Mechanics". John Wiley and Sons, 1989
20. "Guidelines for Design of Dams for Earthquakes". Australian National Committee on Large Dams, 1998
21. Gupta, H. K. "Reservoir Induced Earthquakes", ELSEVIER, 1992
22. "IIT-K GSDMA Guidelines for Seismic Design of Earth Dams and Embankments", IIT-K, GSDMA, 2005
23. "Introduction to Dams". Publication No. 220, Central Board of Irrigation and Power, New Delhi , 1991
24. Jafarzadeh, F. Yaghubi, A. "Three dimensional dynamic behaviour of zoned rockfill dams with emphasis on a real case study". Proc. of the International Symp. On New Trends and Guidelines on Dam Safety/ Barcelona/ Spain/ 17-19 June, 1998
25. Japanese Society of Civil Engineers. "Dynamic Analysis and Earthquake Resistant Design, Vol 1: Strong Motion and Dynamic Properties". Oxford and IBH Publishing Co. Pvt. Ltd, 2000
26. Japanese Society of Civil Engineers. "Dynamic Analysis and Earthquake Resistant Design, Vol 2: Methods of Dynamic Analysis". Oxford and IBH Publishing Co. Pvt. Ltd, 2000
27. Japanese Society of Civil Engineers. "Dynamic Analysis and Earthquake Resistant Design, Vol 3: Dynamic analysis of Special Structures", Dams, Oxford and IBH Publishing Co. Pvt. Ltd., 2000
28. Kjaensli, B., Valstad, J., Hoeg, K. "Rockfill Dams". Norwegian Geotechnical Institute, Hydropower Development, Series 10, 1992
29. Kramer, S. L. "Geotechnical Earthquake Engineering". Prentice Hall, NJ, 1996

30. Kutzner, C. "Earth and Rockfill Dams - Principles of Design and Construction". Oxford and IBH Publishing Co. Pvt. Ltd, 1997
31. Lacy, S. J., Prevost, J. H. "Nonlinear Seismic response analysis of earth dams". Soil Dynamics and Earthquake Engineering, 1987, 6(1), 48-63
32. Lambe, T. W., Whitman, R. V. "Soil Mechanics SI version". John Wiley and Sons, 1979.
33. Mallik, R. K. (2004). "Nonlinear Behaviour of Coupled Bolted Welded Joint of Rapti Bridge", M.Sc. Thesis, Department of Civil Engineering, Pulchowk Campus, IOE, Pulchowk Campus
34. Maskey, P. N. (2005). "Generation of site dependent earthquake ground motion parameters", The Nepalese Journal of Engineering, 1 (1), 84-91
35. Meskouris, K., Konke, C., Chudoba, V.B. "Seismic Safety of Rockfill dams". European Conference on Computational Mechanics, Aug. 31-Sept. 3, 1999, Munchen, Germany.
36. Mircevska, V., Bickovski, V. "Two dimensional nonlinear dynamic analysis of rockfill dam". Proc. of the International Symp. On New Trends and Guidelines on Dam Safety/ Barcelona/ Spain/ 17-19 June, 1998)
37. Murthy, V. N. S. "A Text Book of Soil Mechanics and Foundation Engineering". UBSPD, 1993
38. Newmark, N. M., Rosenblueth, E. "Fundamentals of Earthquake Engineering". Prentice-Hall, Inc, N.J., 1971
39. Ohmachi, T., Kuwano, J. "Dynamic Safety of Earth and Rockfill Dams", A. A. Balkema/Rotterdam, 1994
40. Ozkan, M. Y. "A review of considerations on seismic safety of embankments and earth and rockfill dams". Soil Dynamics and Earthquake Engineering 17(1998), 439-458
41. Pant, K. R. "Significance of RC bands in the out-of-plane vibration of infill masonry walls". M. Sc. Thesis, Department of Civil Engineering, Pulchowk Campus, IOE, Pulchowk Campus, 2005
42. Paz, M. "Structural Dynamics". CBS Publishers and Distributors, New Delhi, 2004

43. "SAP2000 Analysis Reference Manual". Computers and Structures, Inc., Berkeley, California, USA, 2005
44. "Seismic Design and Performance of Dams". Sixteenth Annual USCOLD Lecture Series, Los Angeles, California, July 22-26, 1996
45. "Seismicity and Dam Design". Bulletin 46, CIGB, ICOLD, 1983
46. Shulman, S. G. "Seismic Pressure of water on Hydraulic Structures". Oxford and IBH Publishing Co. Pvt. Ltd, 1990-91
47. Singh, B., Varshney, R. S. "Engineering for Embankment Dams". Oxford and IBH Publishing Co. Pvt. Ltd, 1994
48. Singhal, A. C., Zuroff, M. "Dynamic analysis of dams with nonlinear slip-joints". Soil Dynamics and Earthquake Engineering, 1998, 17, 185-196
49. Smith, L. M., Griffiths, D. V. "Programming the Finite Element Method". John Wiley and Sons, 1998
50. Tani, S. "Behaviour of large fill dams during earthquake and earthquake damage". Soil Dynamics and Earthquake Engineering, 2000, 20, 223-229
51. Uddin, N. "A single step procedure for estimating seismically-induced displacements in earth structures". Computers and Structures, 1997, 64 (5-6), 1175-1182 \*
52. "Upper Karnali Hydroelectric Project". Chapter 7: Seismology, Canadian International Water and Energy Consultants, NEA-Library, Nepal
53. "West - Seti Hydroelectric Project, Local Seismicity Study Report". NEA-Library, Nepal
54. "Workshop on Seismic Analysis and Design of Earth and Rockfill Dams "Volume 1-2, UNDP, Central Soil and Materials Research Station, Central Board of Irrigation and Power, March 21-25 , 1986
55. Zangar, C. N. "Hydrodynamic pressures on dams due to horizontal earthquake effects". Engineering monograph no 11, Bureau of Reclamation, Denver Federal Centre, Denver, Colorado
56. <http://www.liv.ac.uk/seismic/links/info.html>

\* Only abstract available; from the web pages of the corresponding journals.

## **APPENDICES**

# APPENDIX A

## OUTPUT AND REFERENCE FIGURES

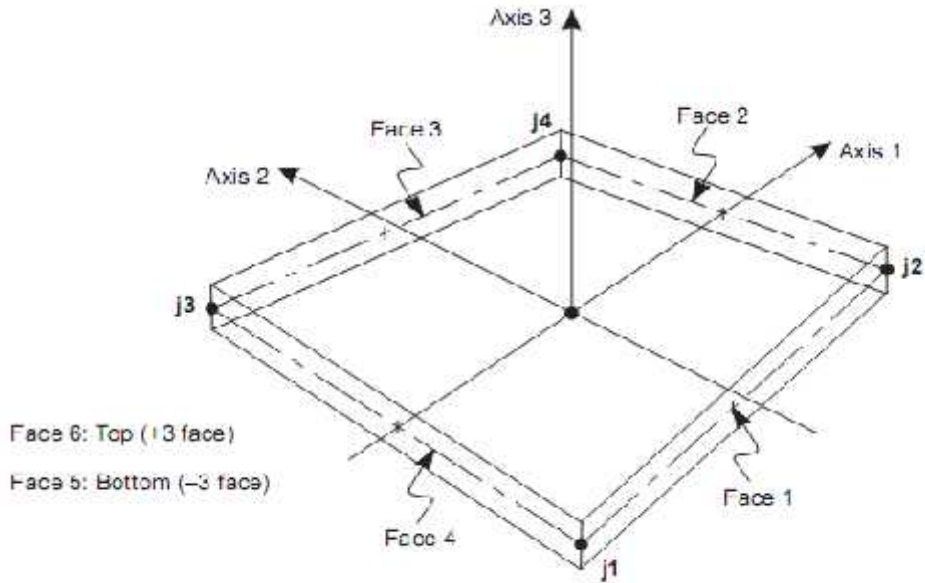


Figure 2.2a: Face definition of quadrilateral element in SAP2000 [43]

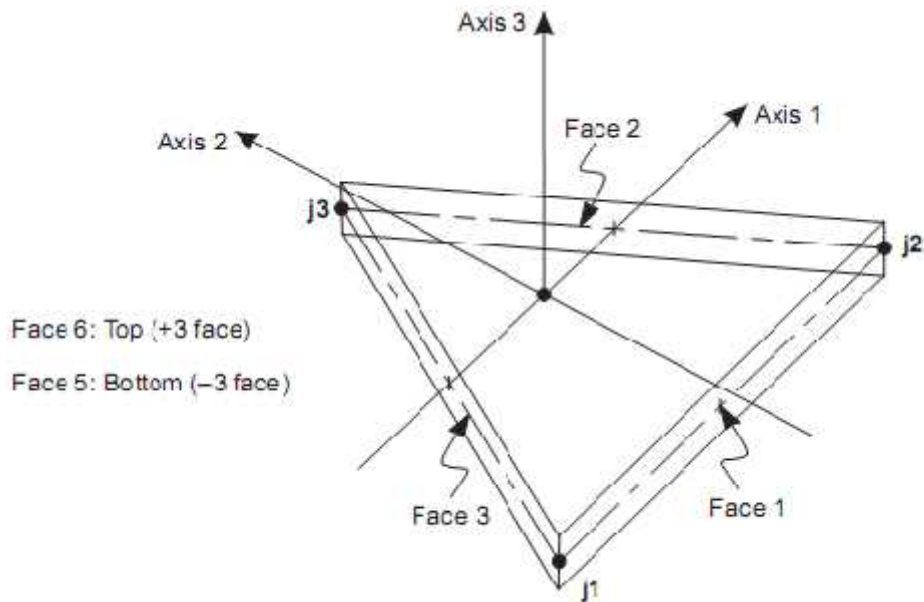
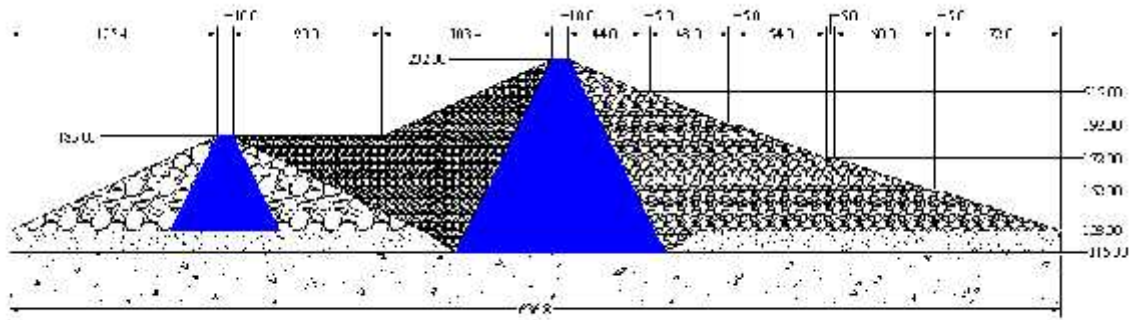


Figure 2.2b: Face definition of triangular element in SAP2000 [43]





TWL = 230.00, FSL = 223.00, MOL = 200.00

- == Impervious Core
- == Rock Fill
- == Gravel Fill
- == Random Fill
- == River Bed Alluvium
- == Rock Line

Figure 3.1: Maximum embankment section of BMP zoned rockfill dam taken for FE modeling (Filters have been incorporated into shells for structural modeling)

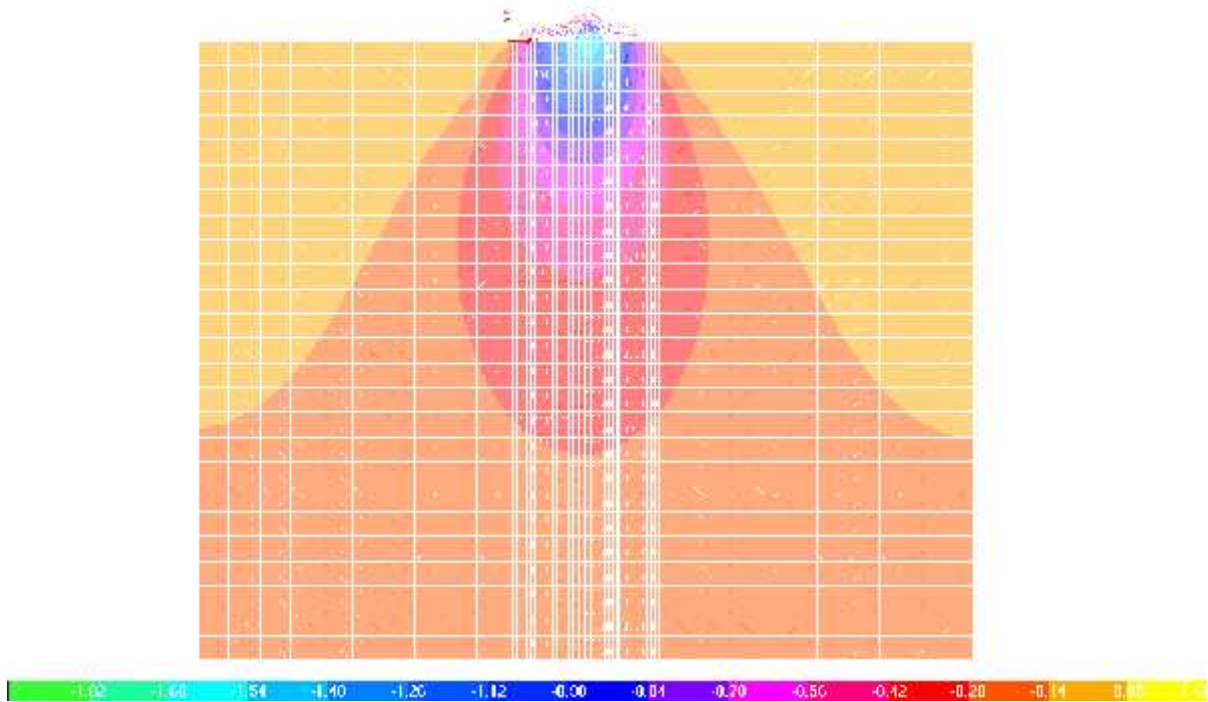


Figure 3.2: A distribution of vertical foundation stresses (pressure bulb) under gravity turn-on load; during the trial procedure of fixing the effective foundation geometry

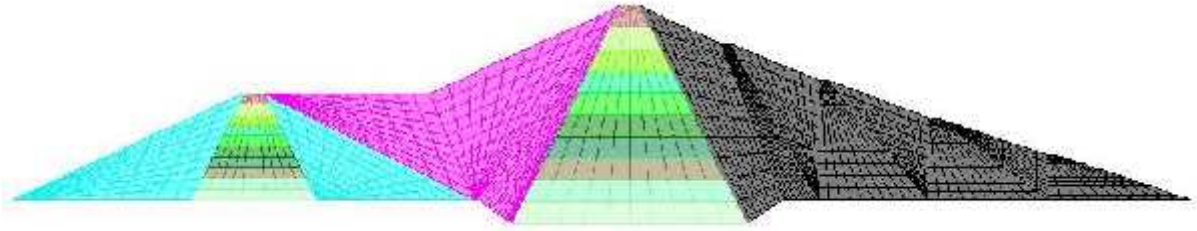


Figure 3.3: 2D finite element model of BMP zoned rockfill dam with rigid foundation (RF model)

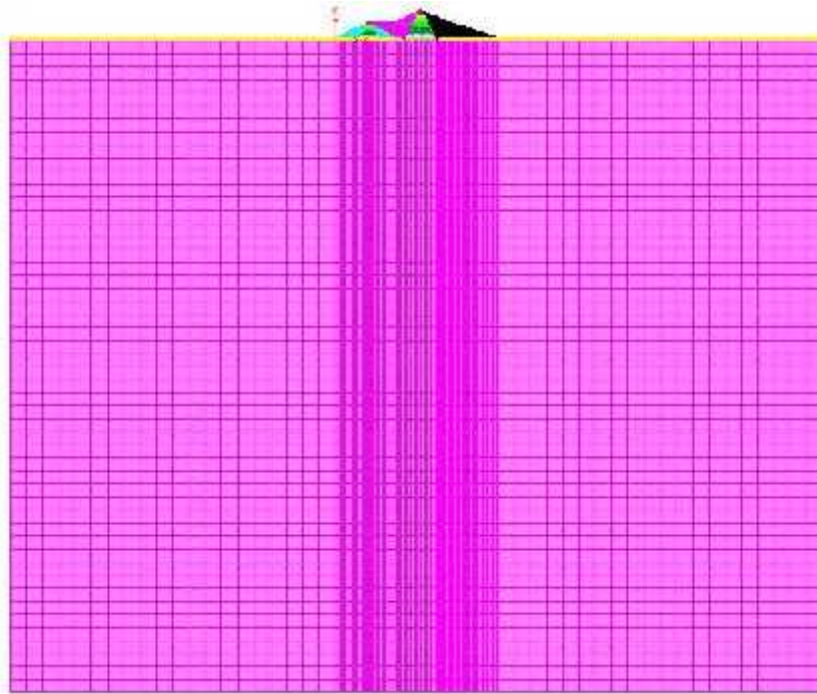


Figure 3.4a: 2D finite element model of BMP zoned rockfill dam with flexible foundation (FF model)

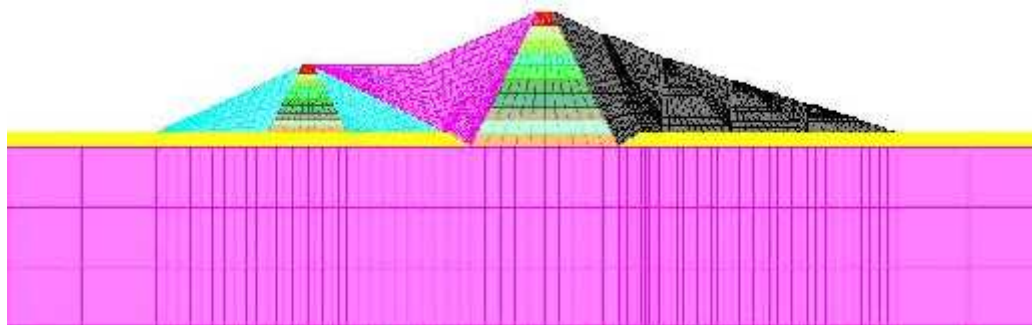


Figure 3.4b: FF model with dam section zoomed

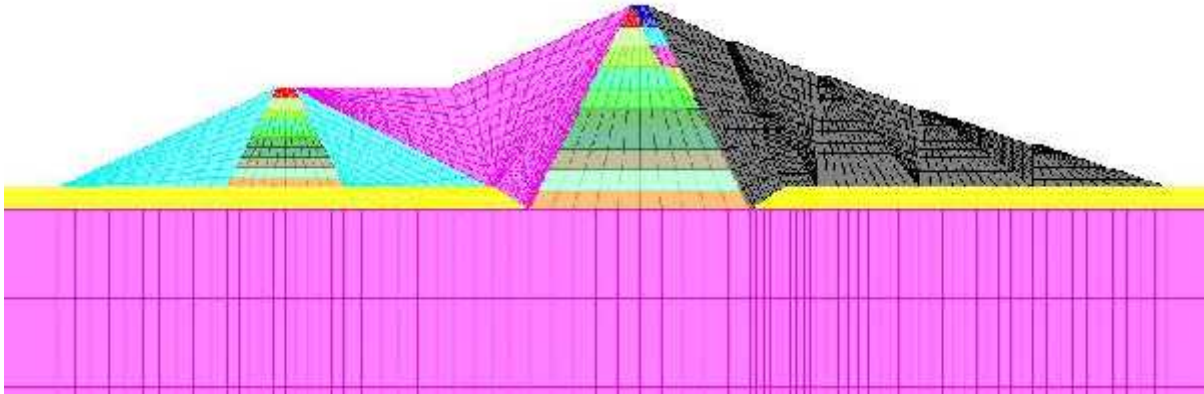
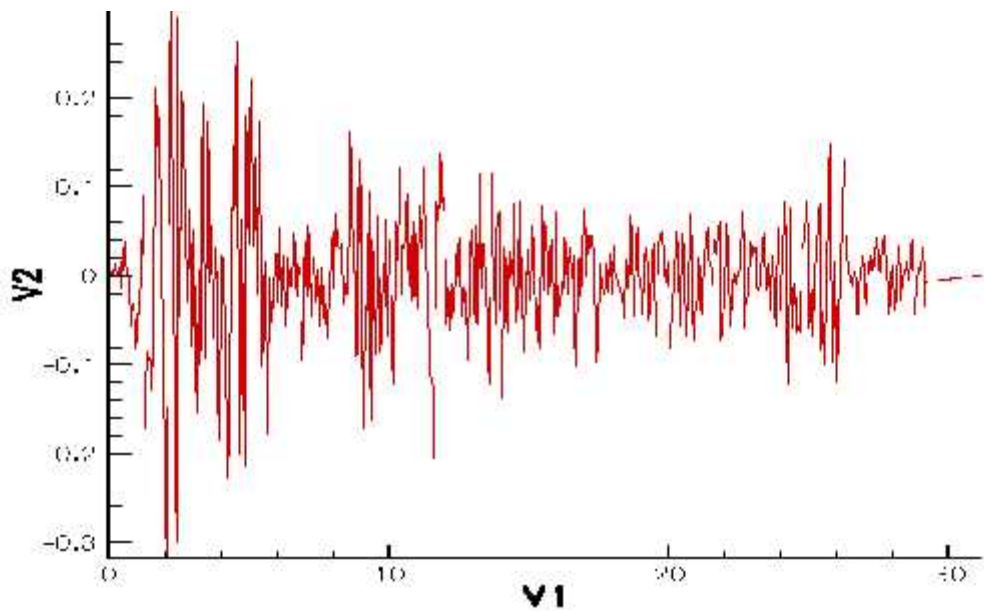
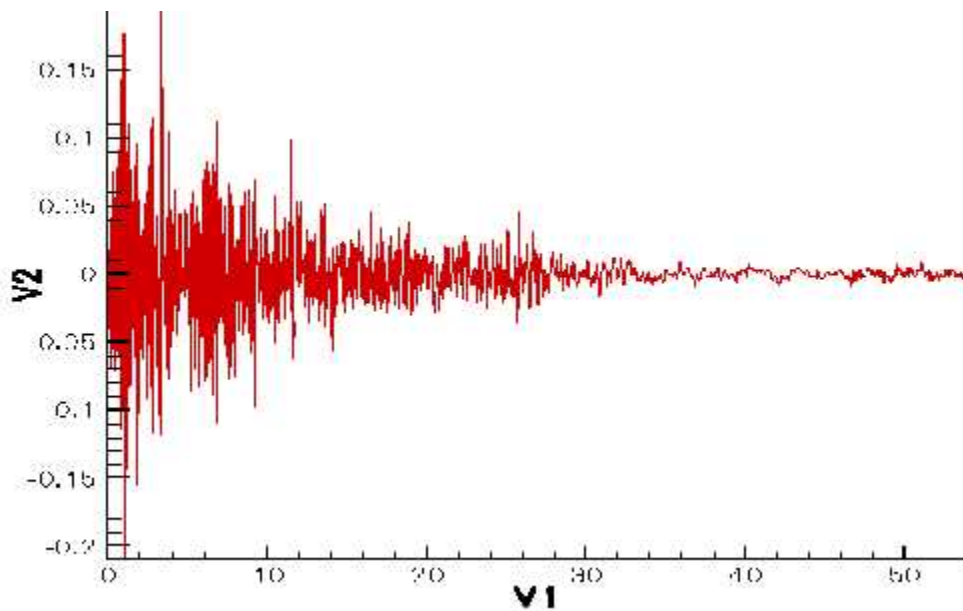


Figure 3.5: Division of core into saturated and dry parts by the phreatic line; shown in FF\_WR model, with dam section zoomed



a) N- S component

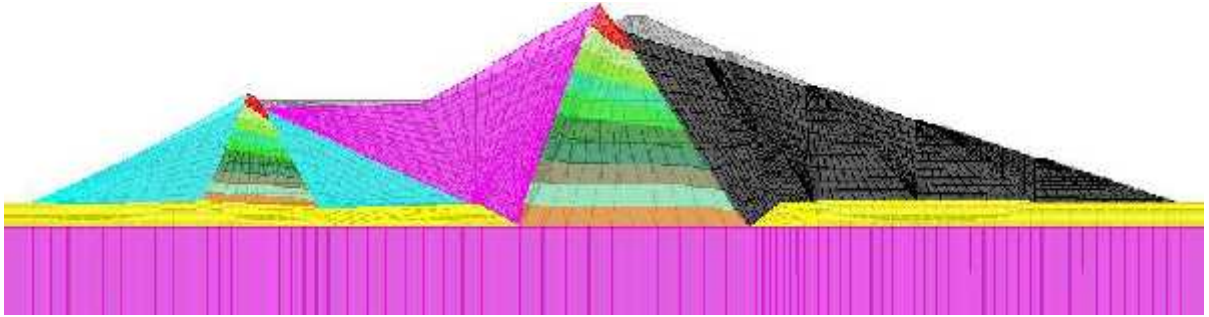


b) Vertical component

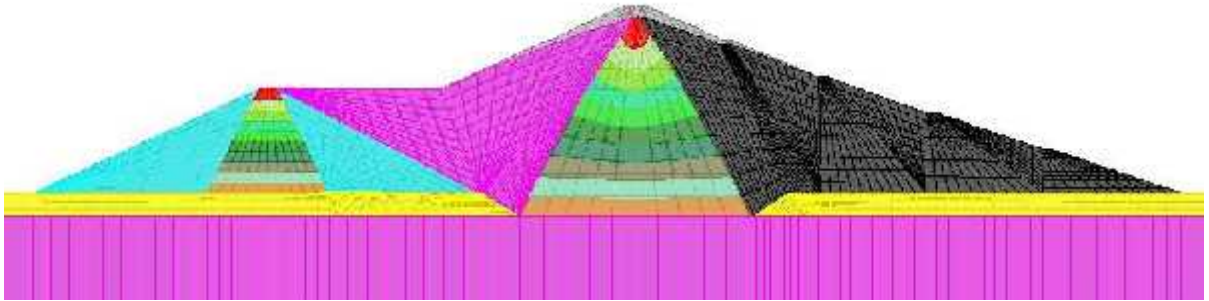
V1 = Time (sec)

V2 = Ground acceleration component in units of g

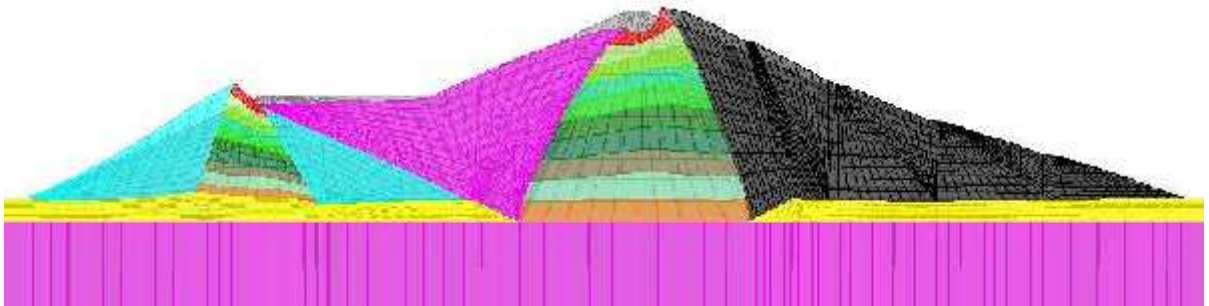
Figure 3.6: The recorded a) N-S, and b) vertical acceleration components of El Centro earthquake; taken as prescribed input ground motion [Courtesy: USGS]



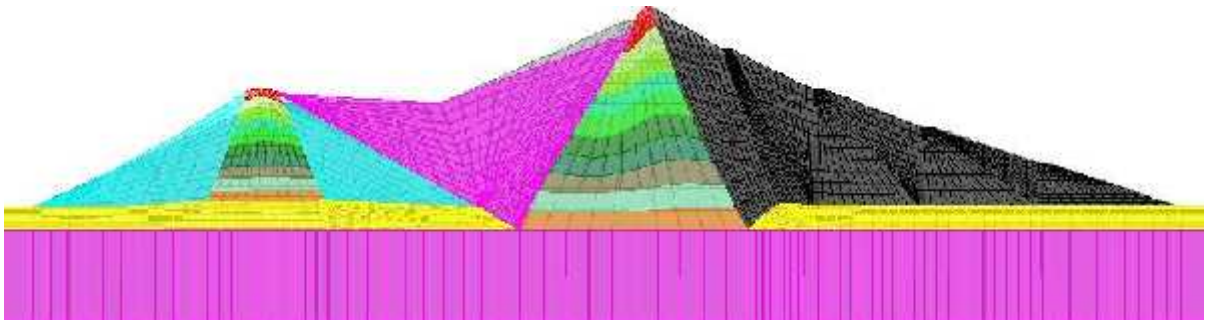
a) Mode 1 (T = 1.1957 Sec)



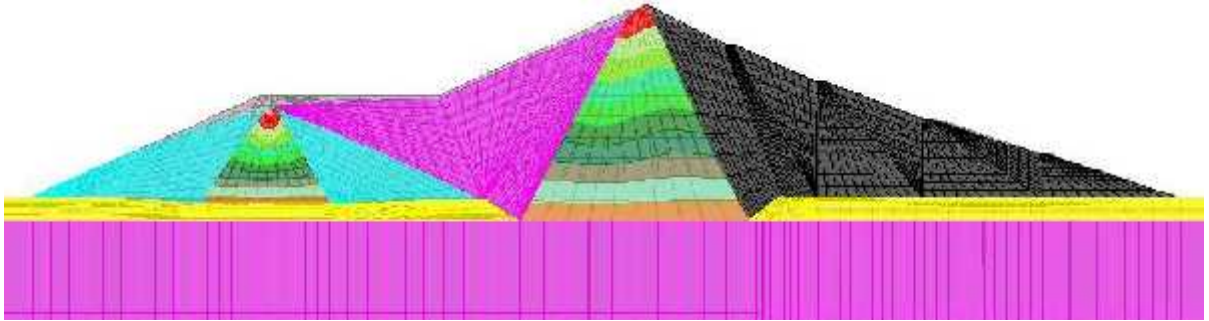
b) Mode 2 (T = 0.9343 Sec)



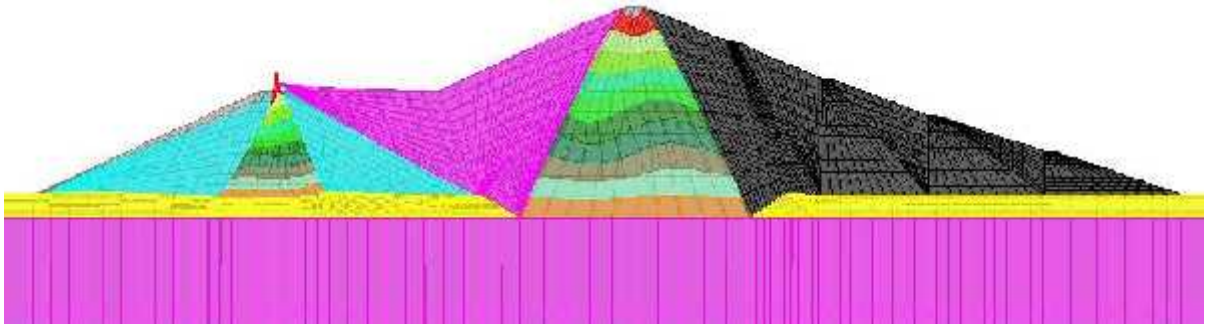
c) Mode 3 (T = 0.8068 Sec)



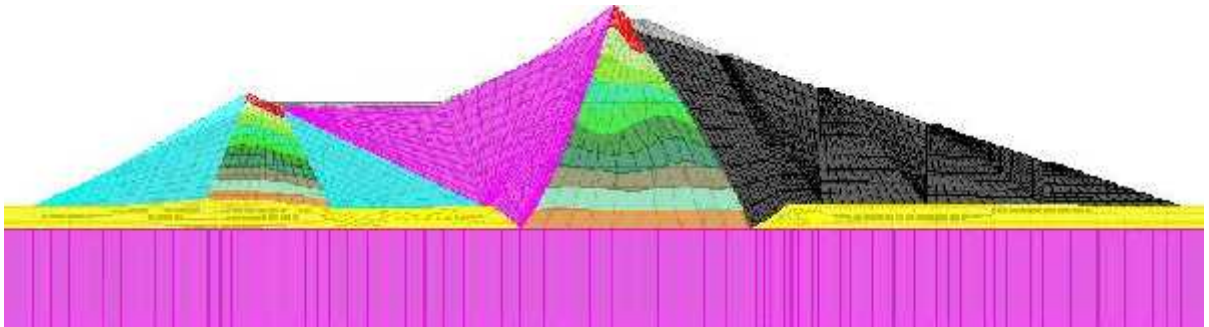
d) Mode 4 (T = 0.7031 Sec)



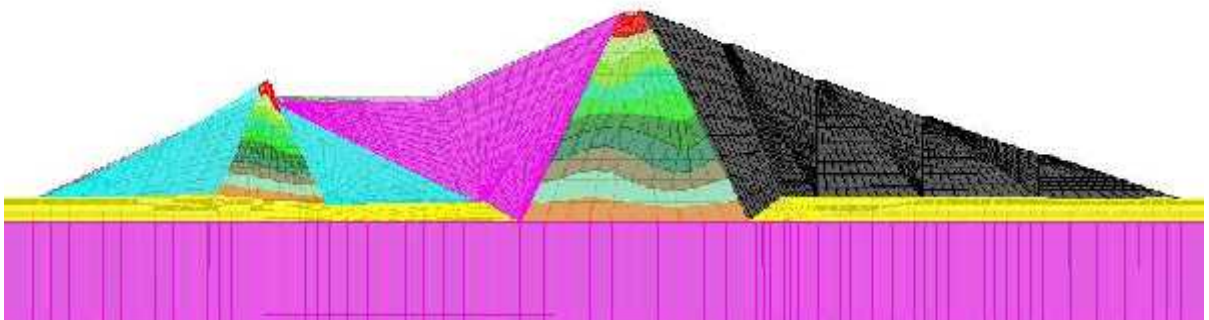
e) Mode 5 (T = 0.6728 Sec)



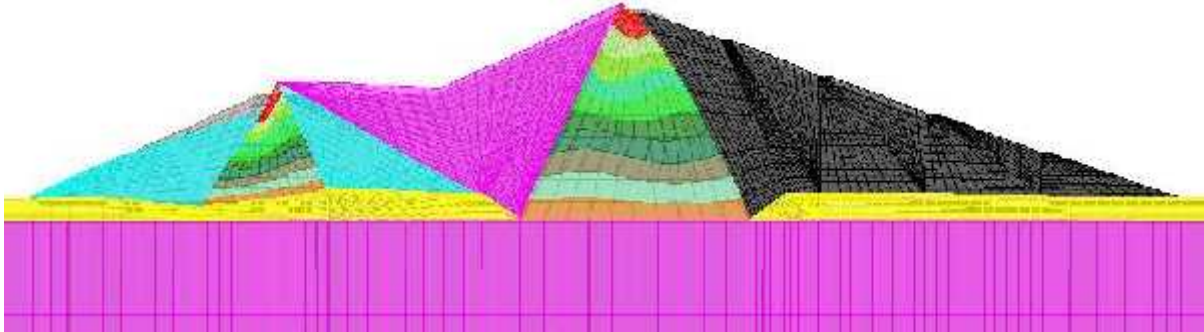
f) Mode 6 (T = 0.6318 Sec)



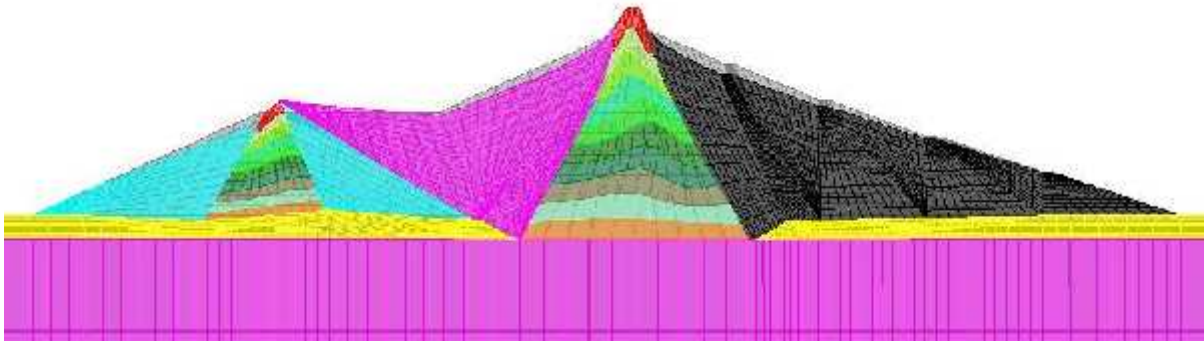
g) Mode 7 (T = 0.6060 Sec)



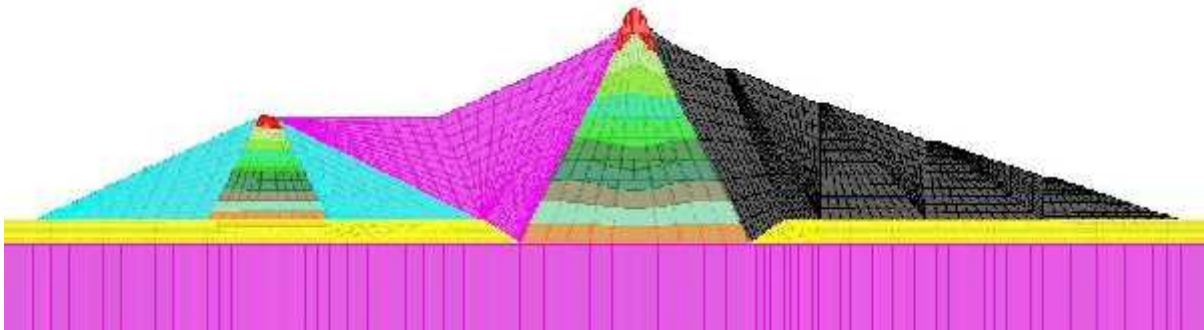
h) Mode 8 (T = 0.5713 Sec)



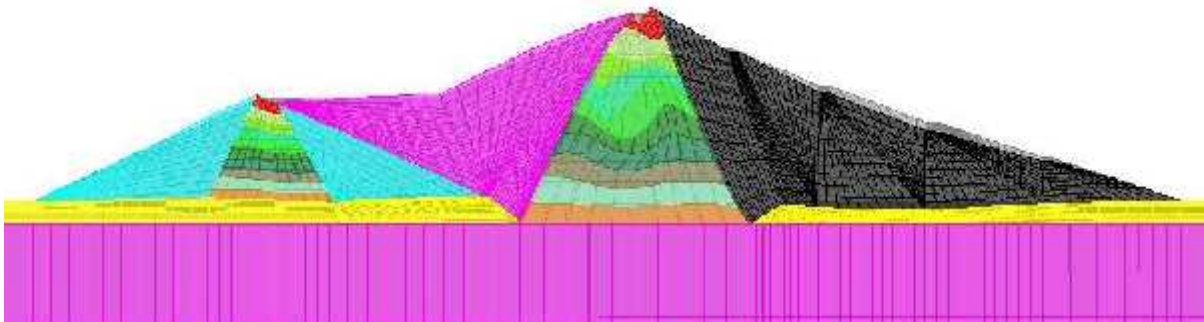
i) Mode 9 (T = 0.5557 Sec)



j) Mode 10 (T = 0.5414 Sec)



k) Mode 11 (T = 0.5172 Sec)



l) Mode 12 (T = 0.4981 Sec)

Figure 4.1: First twelve significant mode shapes of BMP zoned dam with FF model (a –l)

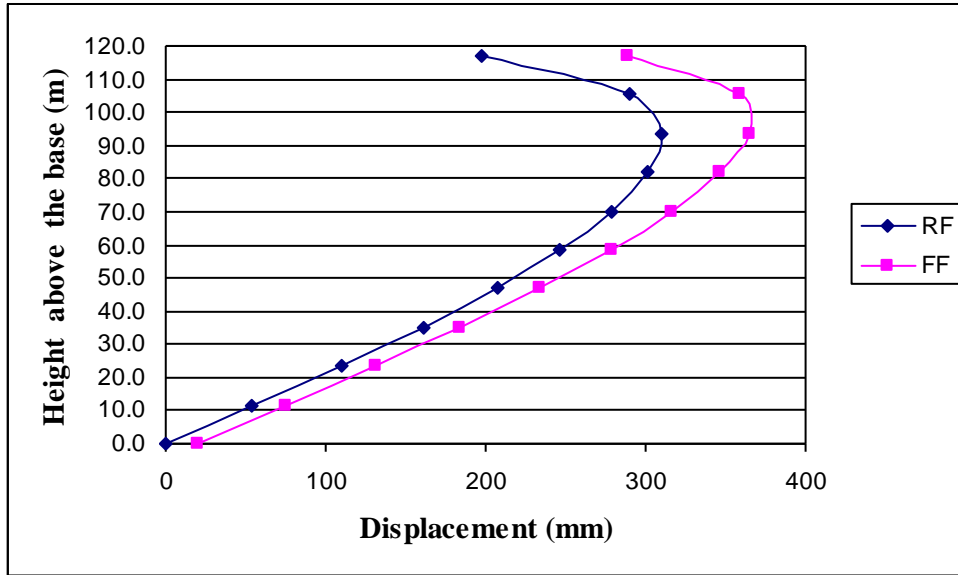


Figure 4.2a: Vertical displacement (settlement) profile of core along a vertical through the core centre; due to gravity turn-on load

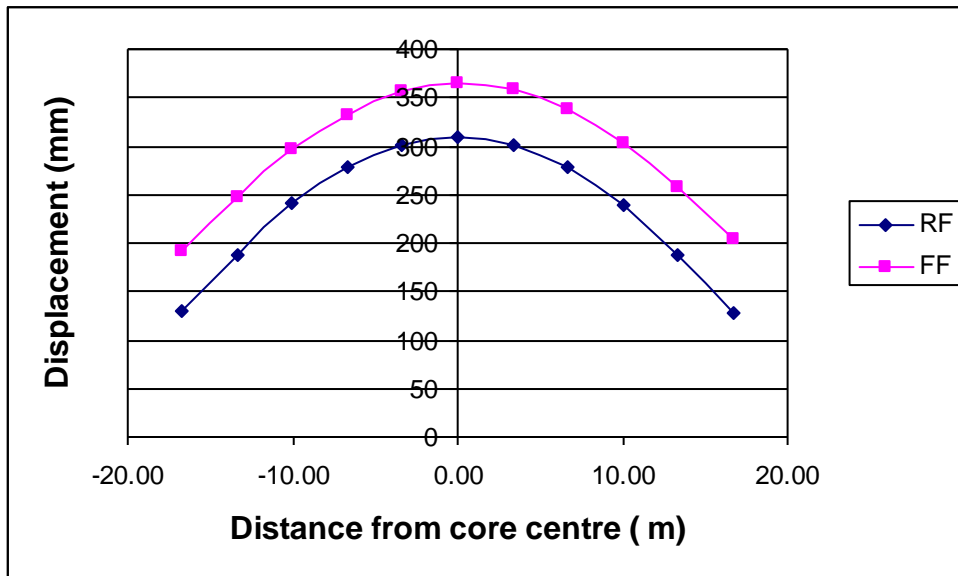


Figure 4.2b: Vertical displacement (settlement) profile of core along the horizontal line at the height of maximum settlement (93.6 m); due to gravity turn-on load



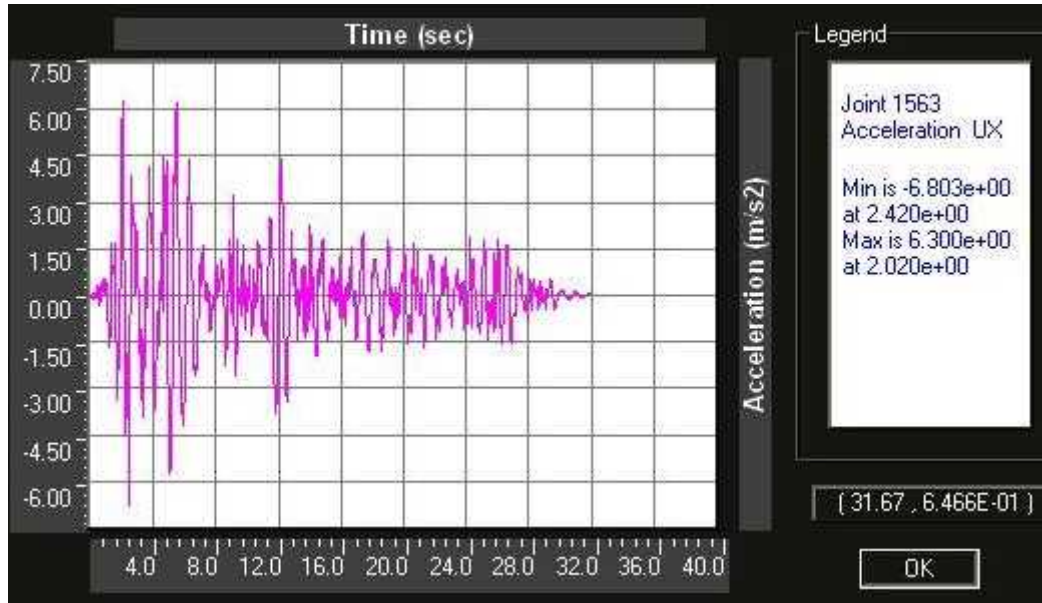


Figure 4.3a: Response acceleration history at the crest of RF\_WOR model

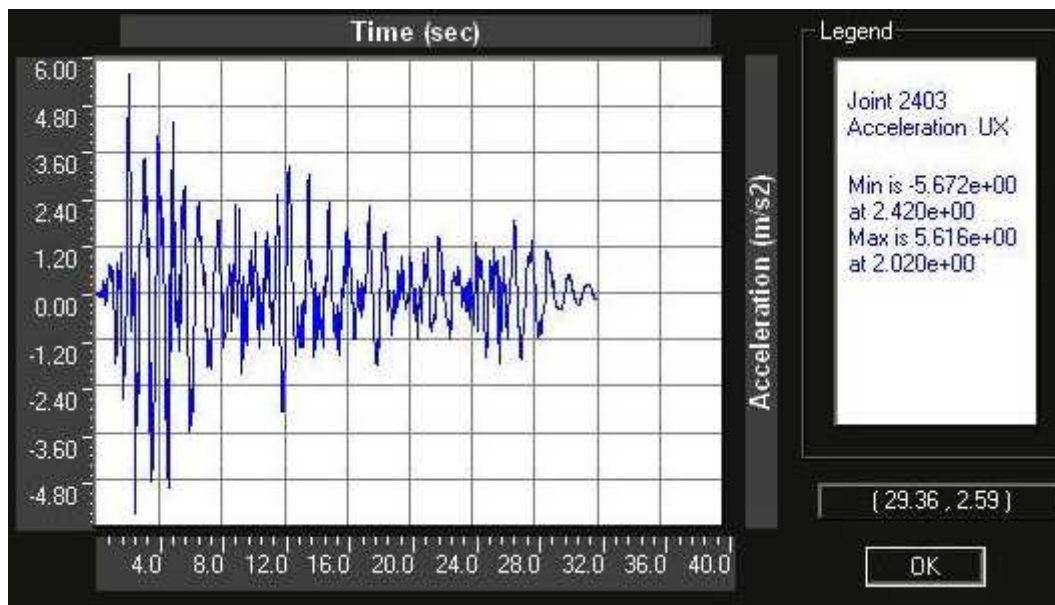


Figure 4.3b: Response acceleration history at the crest of FF\_WOR model

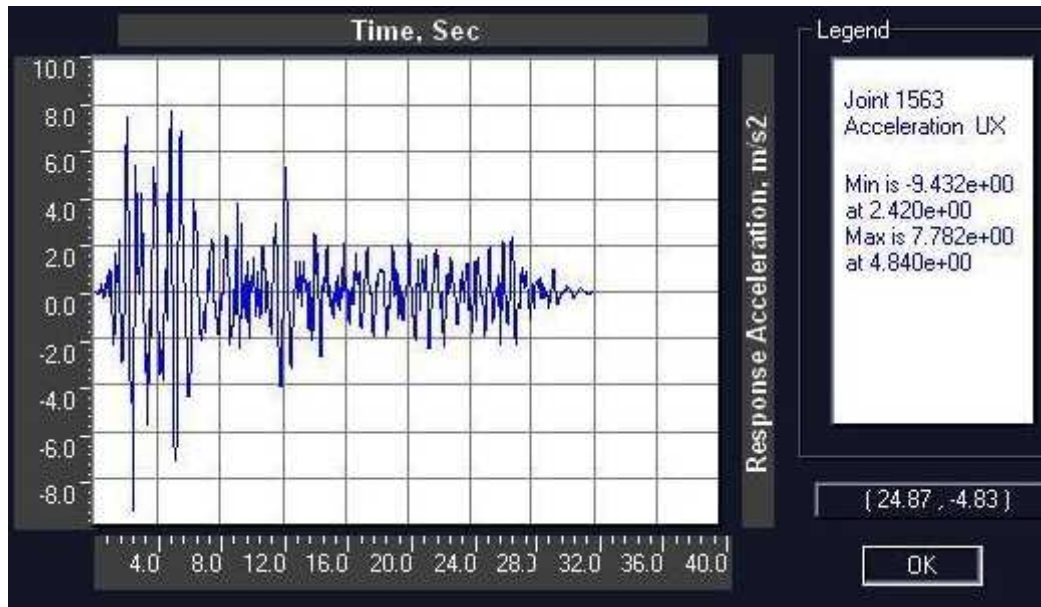


Figure 4.3c: Response acceleration history at the crest of RF\_WR model

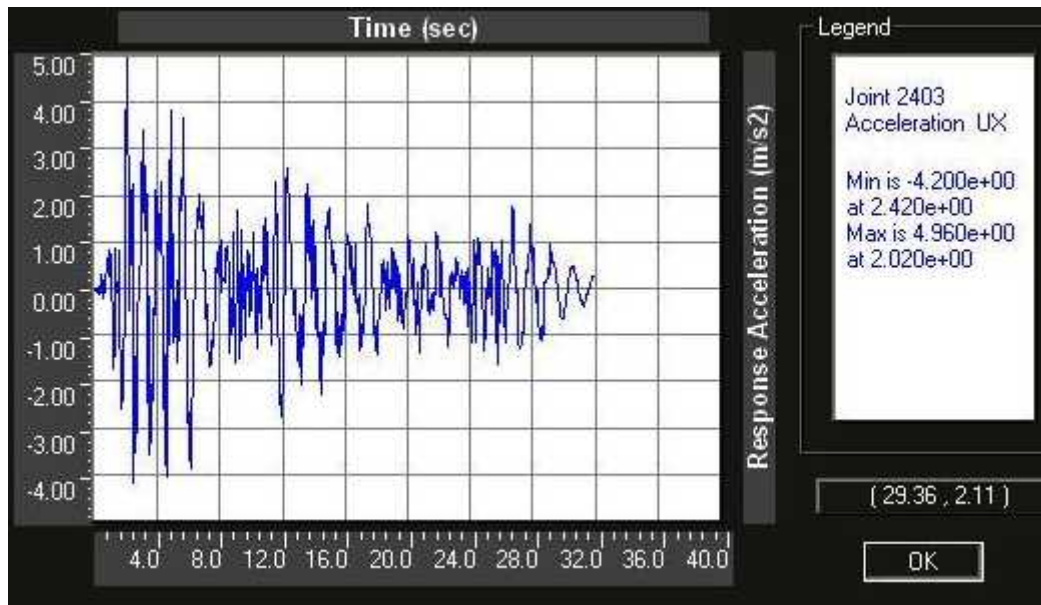


Figure 4.3d: Response acceleration history at the crest of FF\_WR model

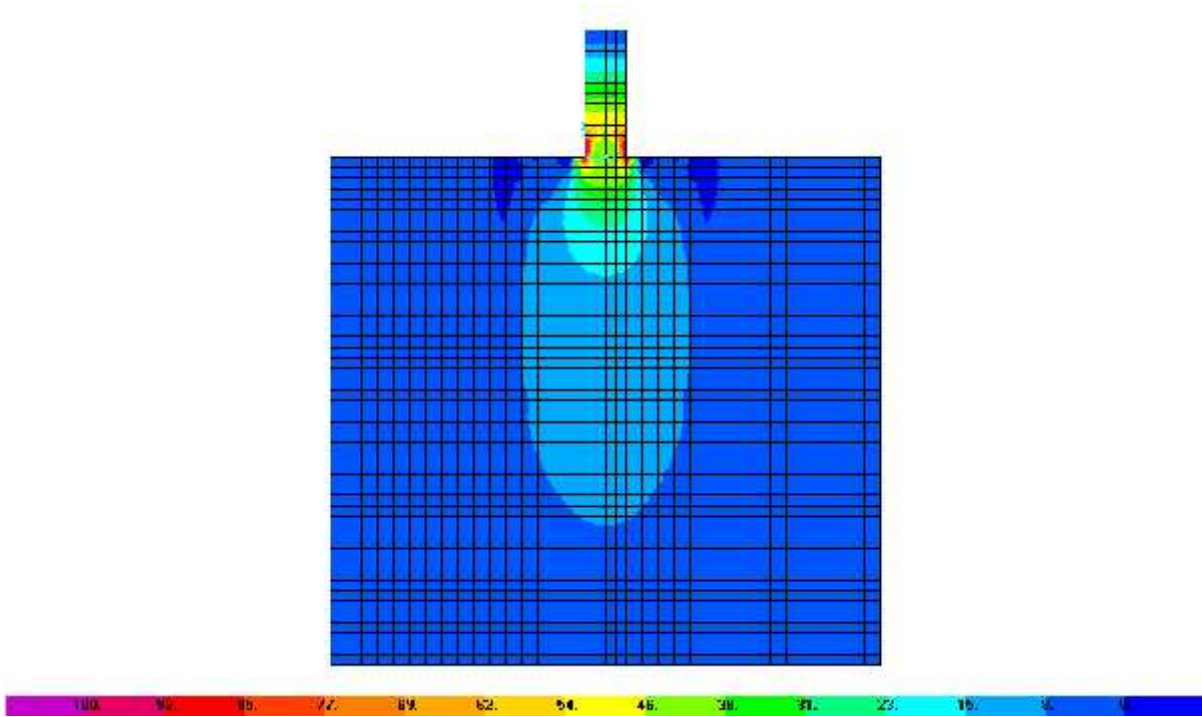
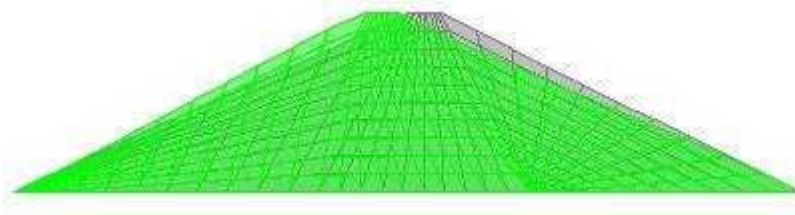
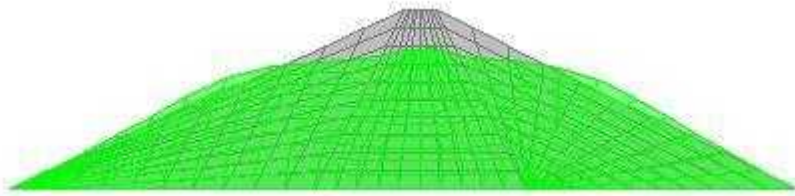


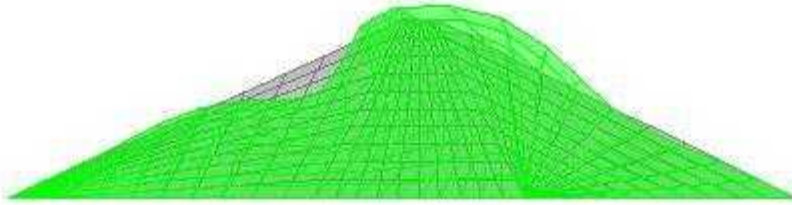
Figure 5.1: Foundation stress distribution for a model wall taken



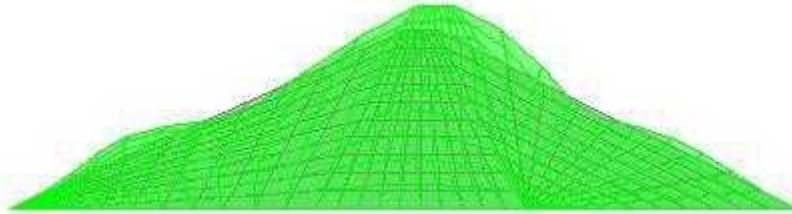
a) Mode 1 (T = 0.228 Sec)



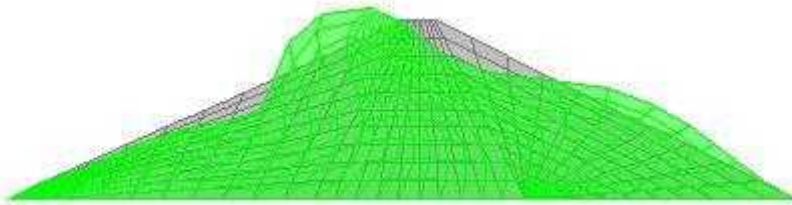
b) Mode 2 (T = 0.149 Sec)



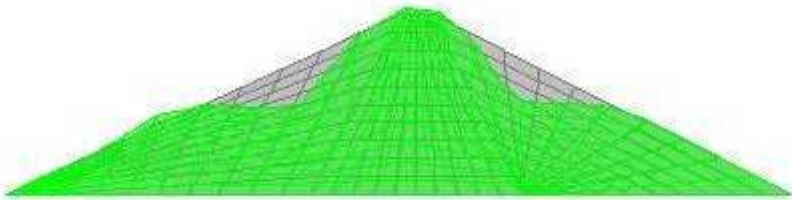
c) Mode 3 (T = 0.128 Sec)



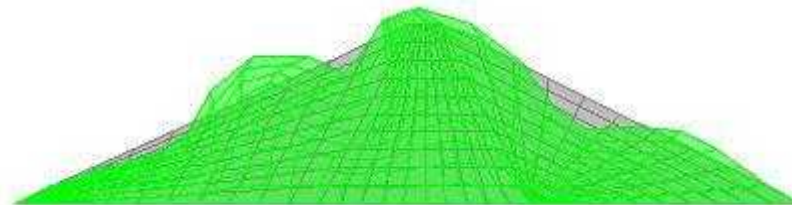
d) Mode 4 (T = 0.107 Sec)



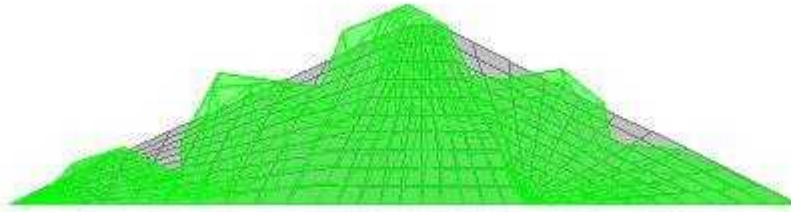
e) Mode 5 (T = 0.103 Sec)



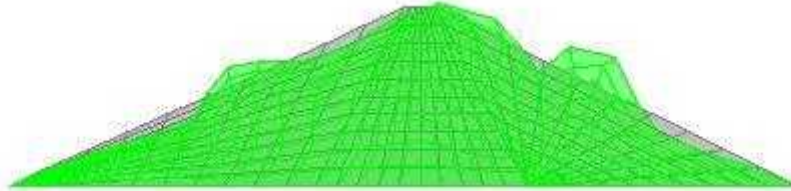
f) Mode 6 (T = 0.099 Sec)



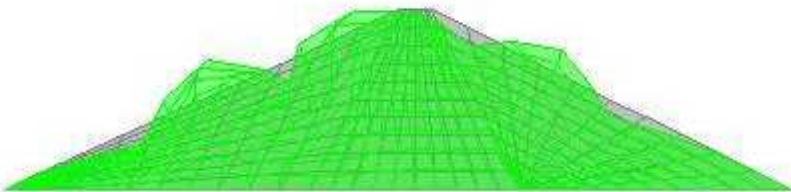
g) Mode 7 (T = 0.091 Sec)



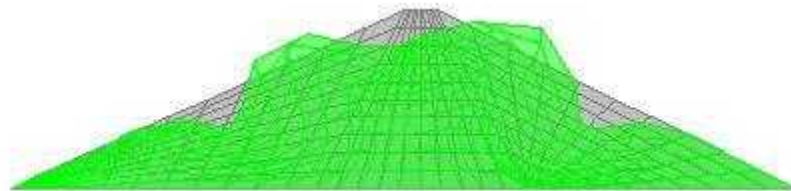
h) Mode 8 (T = 0.086 Sec)



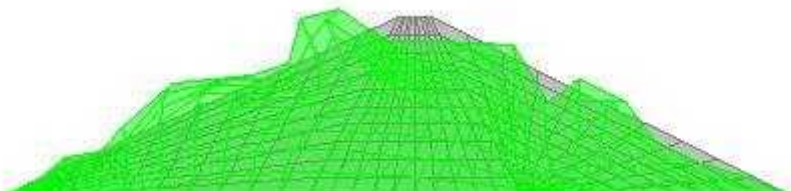
i) Mode 9 (T = 0.079 Sec)



j) Mode 10 (T = 0.075 Sec)

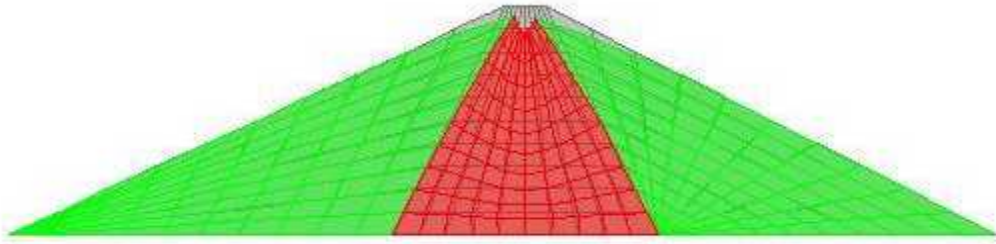


k) Mode 11 (T = 0.071 Sec)

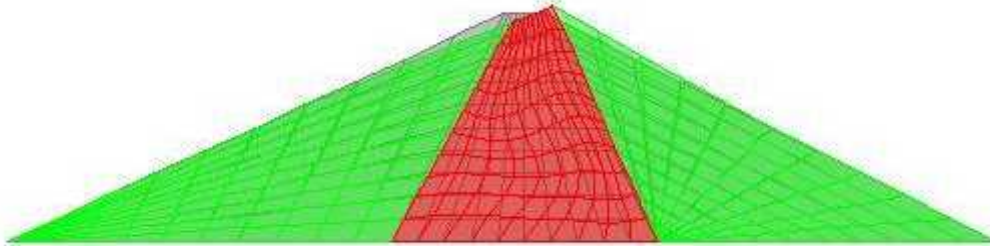


l) Mode 12 (T = 0.070 Sec)

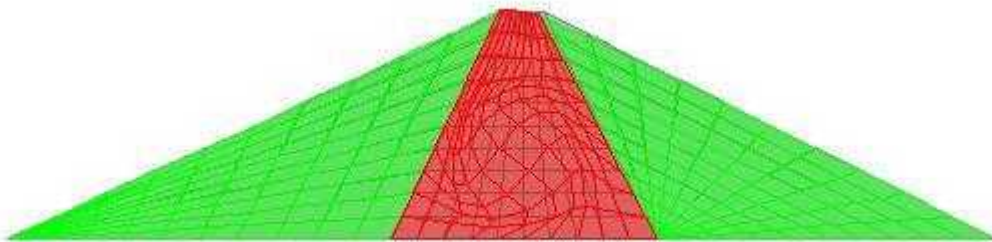
Figure 5.2: Vibration modes of the model symmetrical homogeneous rockfill dam (a-l)  
(Height = 57 m, E = 3000 MPa,  $\nu = 0.38$ )



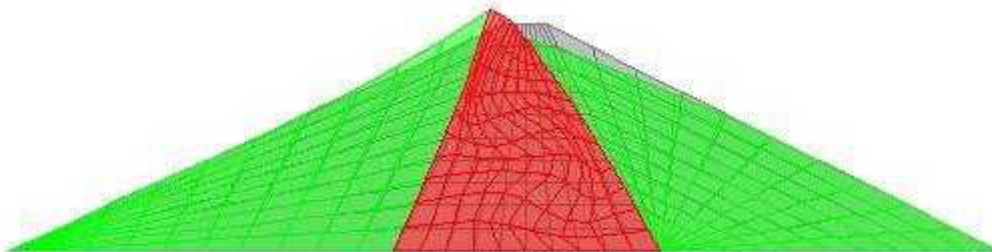
a) Mode 1 ( $T = 0.786$  Sec)



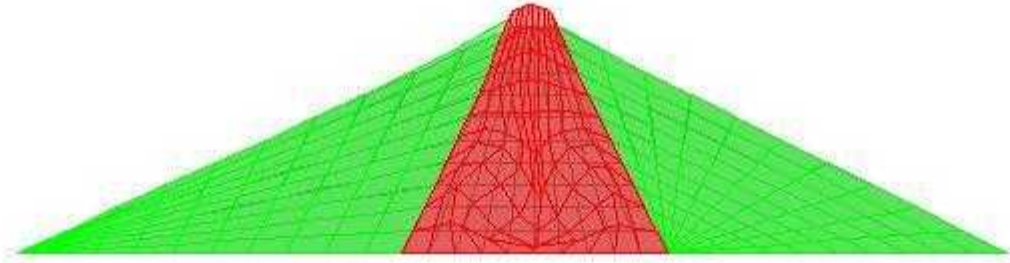
b) Mode 2 ( $T = 0.663$  Sec)



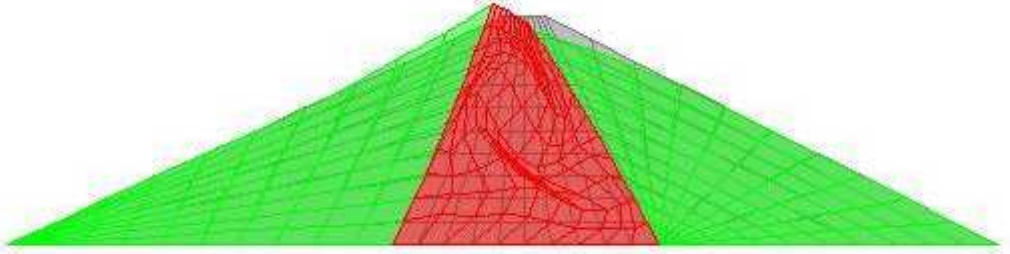
c) Mode 3 ( $T = 0.653$  Sec)



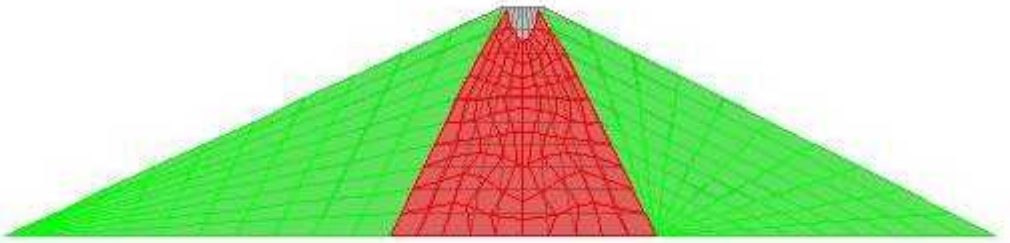
d) Mode 4 ( $T = 0.521$  Sec)



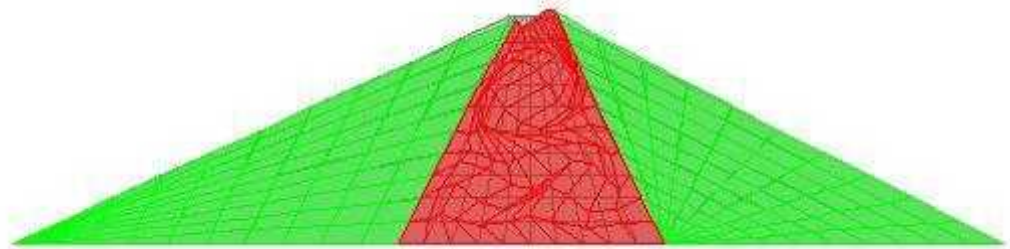
e) Mode 5 ( $T = 0.517$  Sec)



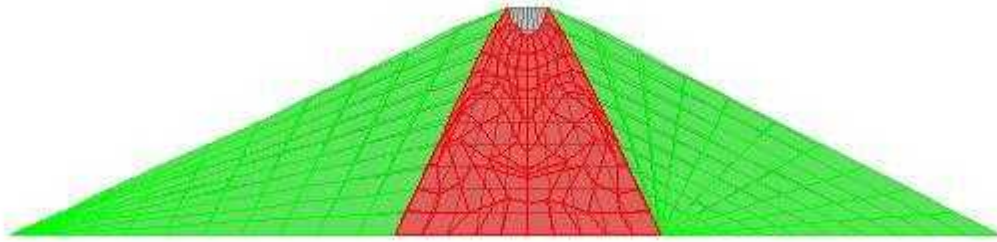
f) Mode 6 ( $T = 0.497$  Sec)



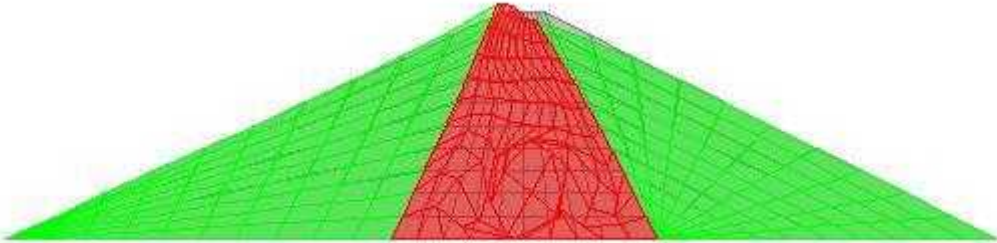
g) Mode 7 ( $T = 0.439$  Sec)



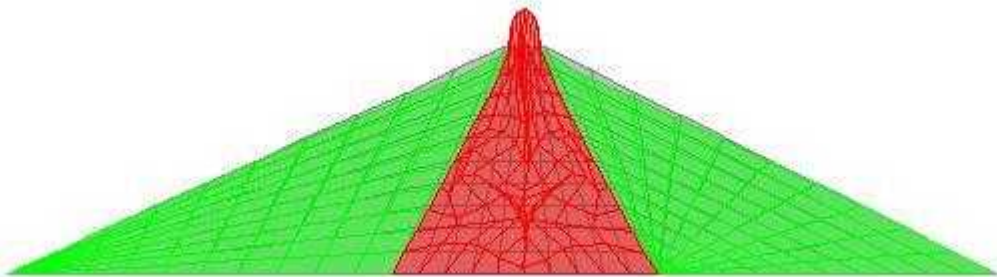
h) Mode 8 ( $T = 0.434$  Sec)



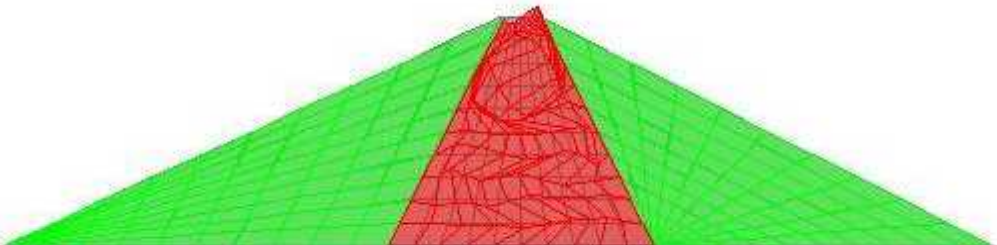
i) Mode 9 (T = 0.430 Sec)



j) Mode 10 (T = 0.422 Sec)



k) Mode 11 (T = 0.382 Sec)



l) Mode 12 (T = 0.381 Sec)

Figure 5.3: Vibration modes of the model symmetrical zoned rockfill dam  
(E = 3000 MPa,  $\nu = 0.38$  for shell; and E= 20 MPa,  $\nu = 0.42$  for core)



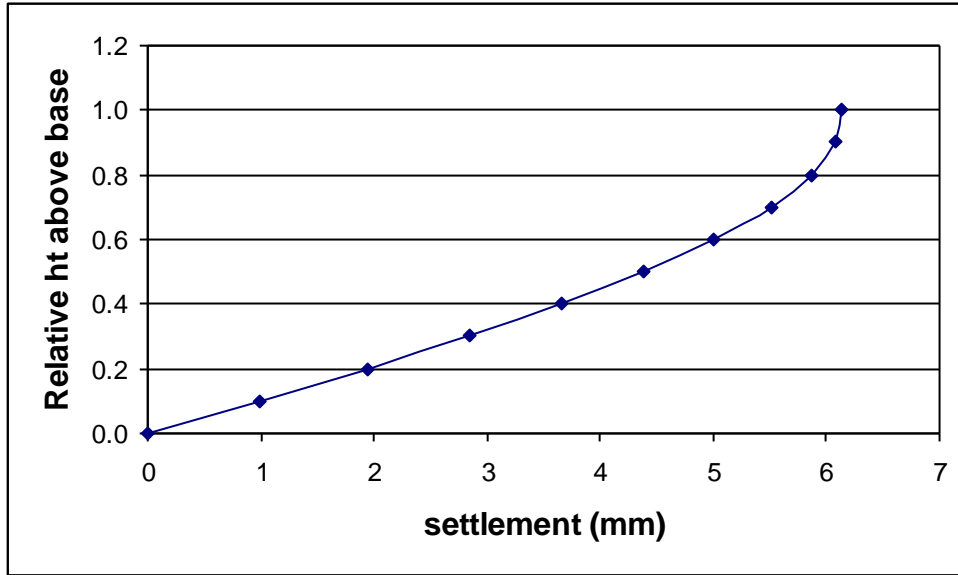


Figure 5.4: Settlement profile along a vertical through the centre of core of a model symmetrical homogeneous rockfill dam

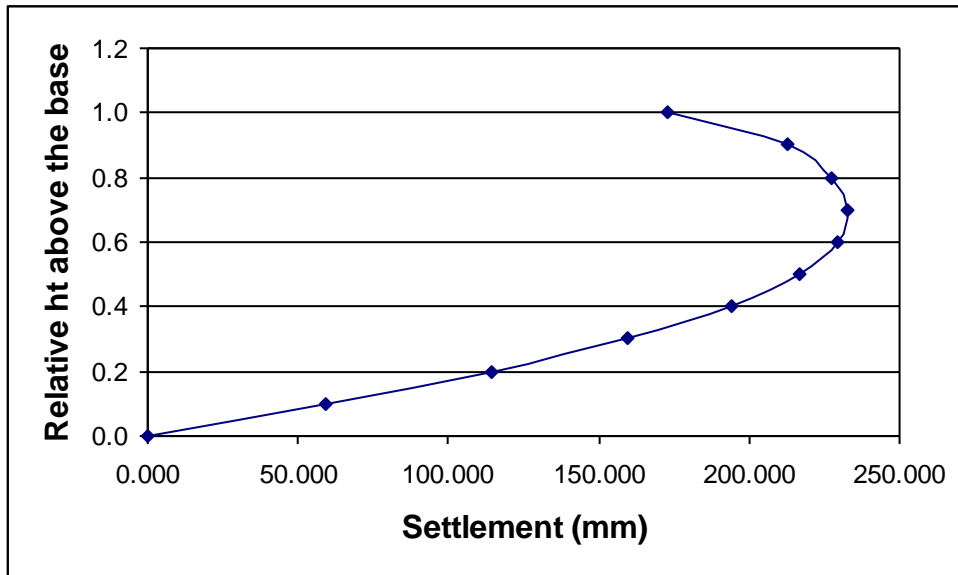
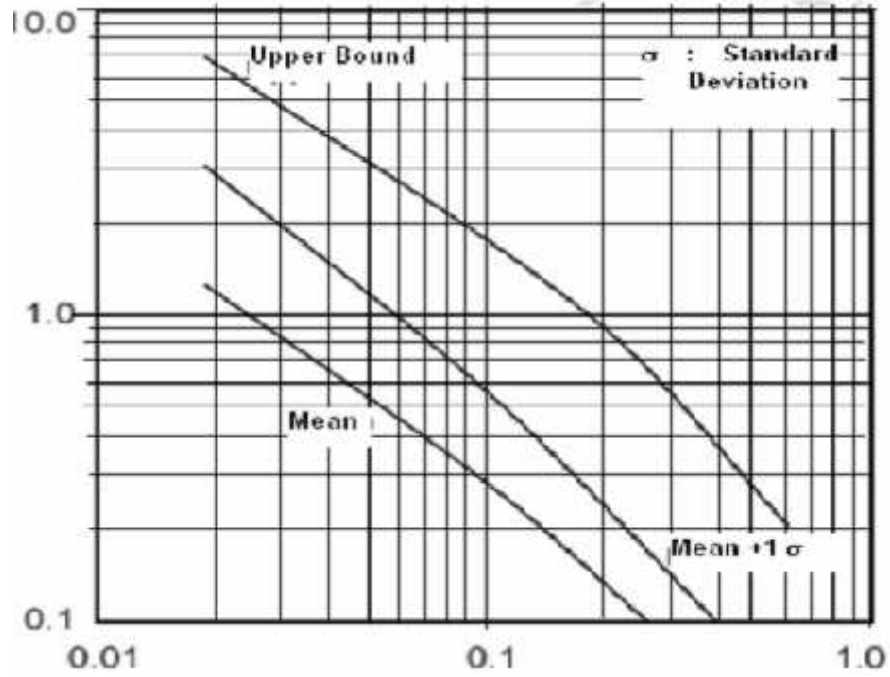


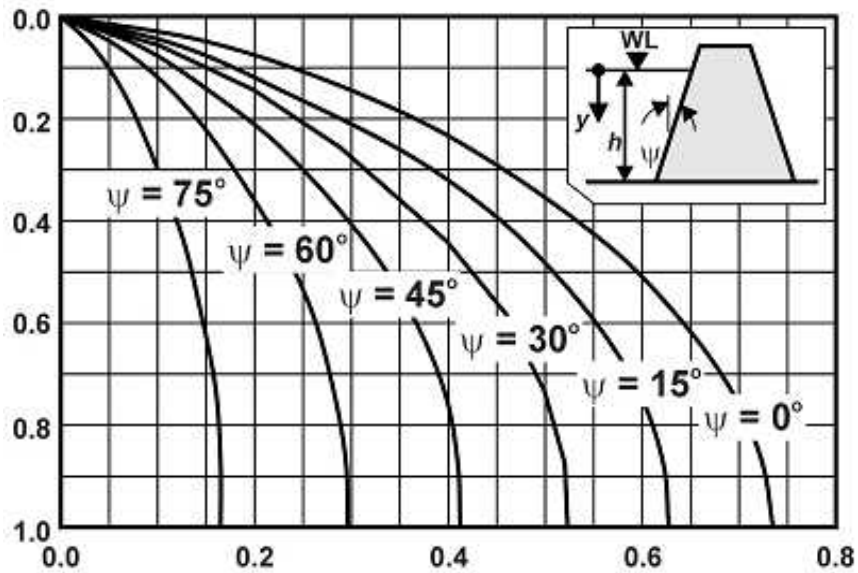
Figure 5.5: Settlement profile along a vertical through the centre of core of a model symmetrical zoned rockfill dam



Horizontal axis = acceleration / Peak response acceleration

Vertical axis = Permanent displacement in meters

Figure 5.6: Chart given in IS guidelines to estimate the permanent displacement [22]



Horizontal axis =Hydrodynamic pressure coefficient (C), Vertical axis =  $y/h$

Figure C.1: Chart given in IS guidelines for the hydrodynamic pressure coefficient [22]

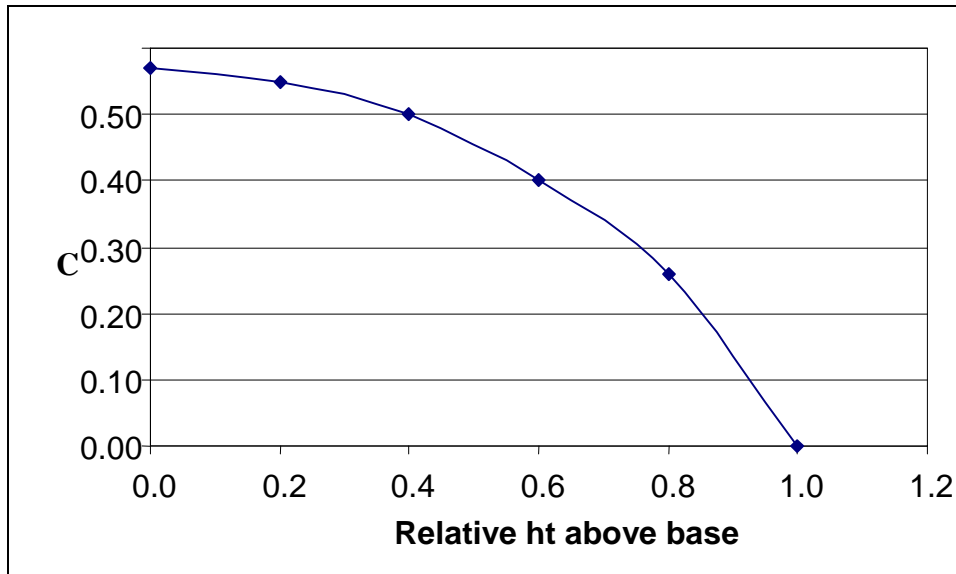


Figure C.2: Plot of hydrodynamic pressure coefficient for BMP dam cores

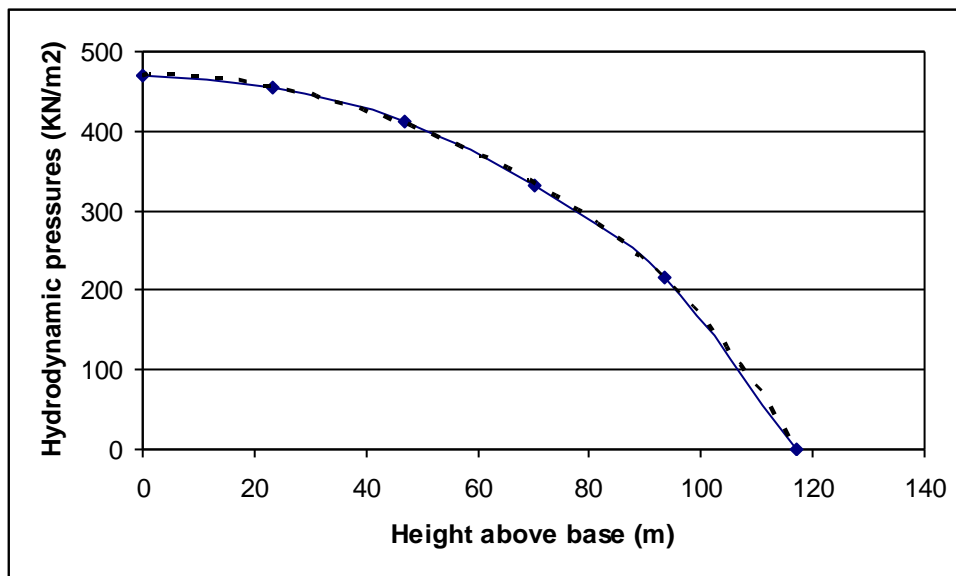


Figure C.3a: Plot of hydrodynamic pressure on main dam core, and the best fit curve

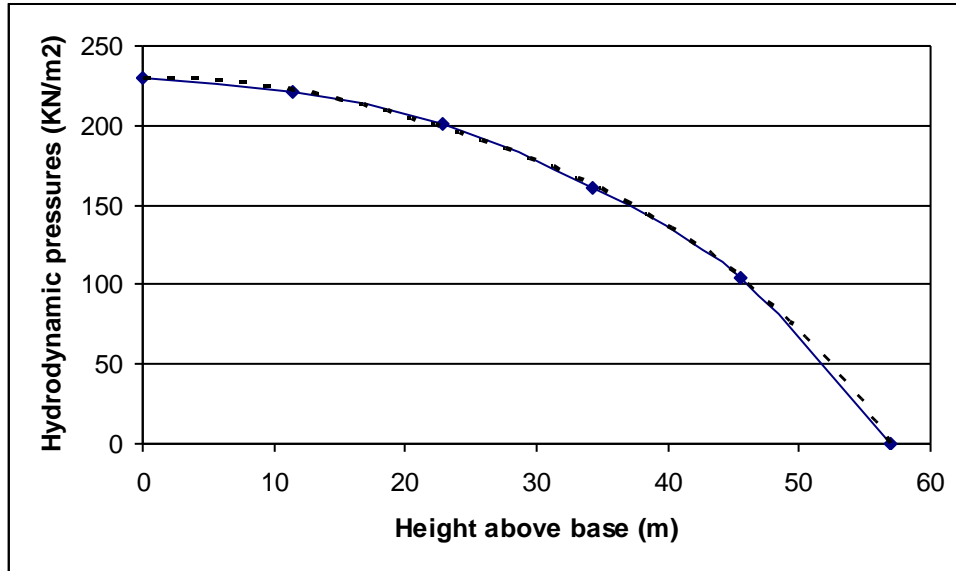


Figure C.3b: Plot of hydrodynamic pressure on coffer dam core, and the best fit curve

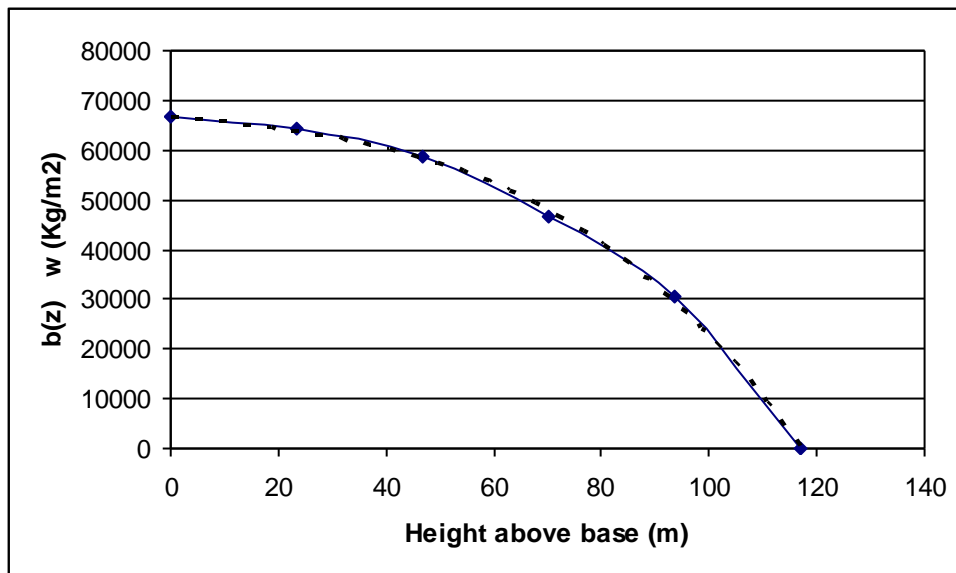


Figure C.4a: Plot of shape of equivalent hydrodynamic added reservoir for main dam- core, multiplied by  $w$

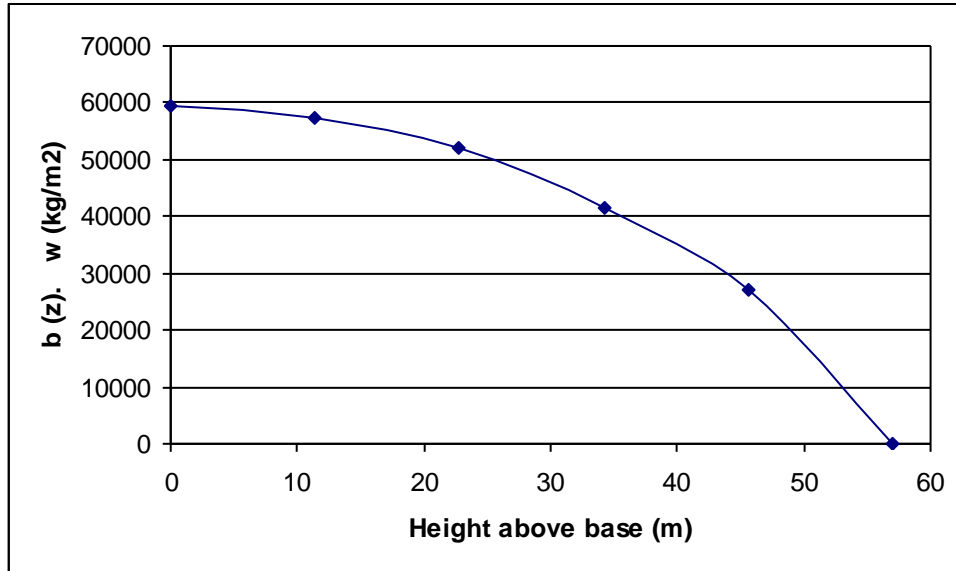
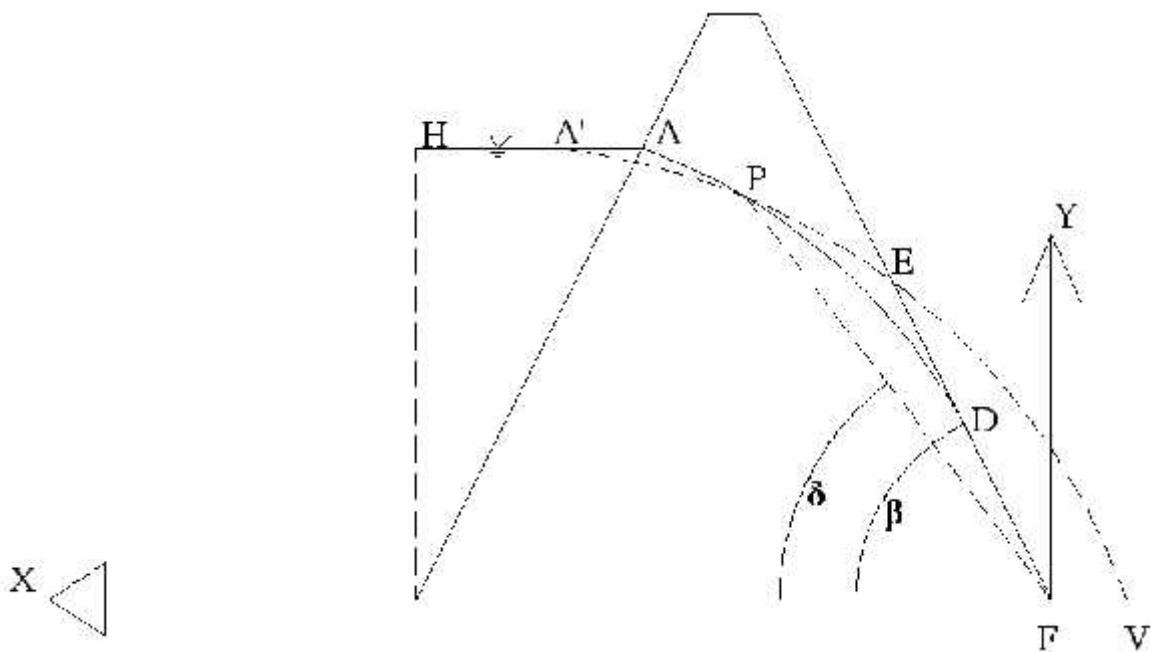


Figure C.4 b: Plot of shape of equivalent hydrodynamic added reservoir for coffer dam- core, multiplied by  $w$



$$AH = m, AA' = 0.3m, FP = r, FD = a, ED = a$$

$A'PEV$  = Basic parabola,  $APD$  = corrected phreatic line

Figure D.1: Phreatic line location in an earthen dam

## APPENDIX B

### OUTPUT TABLES

Table 3.1: Material - unit weights (KN/m<sup>3</sup>)

Material Type	Dry (Unsaturated) state	Saturated state
Rock Fill- Shell	19.90	22.10
Gravel Fill- Shell	18.50	20.00
Random Fill- Shell	18.50	20.00
Rolled Clay- Core	19.80	20.60
Alluvial- Foundation	19.50	21.50
Rock- Foundation	21.00	-

Table 3.2: Unsaturated materials - elastic constants (E in N/mm<sup>2</sup>)

Material Type	E	
Rock Foundation	50,000	0.35
Alluvial Foundation	150	0.38
Shells	3,000	0.25
Core in the order of depth below crest	1/10	0.42
	2/10	0.42
	3/10	0.42
	4/10	0.42
	5/10	0.42
	6/10	0.42
	7/10	0.42
	8/10	0.42
	9/10	0.42
	10/10	0.42

Table 3.3: Hydrodynamic added forces (KN)

Relative ht. above base	For Main Dam	For Cofferdam
0.1	5509.798	337.797
0.2	5426.642	332.506
0.3	5245.564	320.645
0.4	5002.452	303.934
0.5	4717.409	283.035
0.6	4394.753	257.557
0.7	4023.014	226.056
0.8	3574.900	186.034
0.9	3007.491	133.941
1.0	2261.842	65.166

Table 3.4: Hydrodynamic added masses (KN-s<sup>2</sup>/m)

Relative ht. above base	For Main Dam	For Cofferdam
0.1	774.620	185.139
0.2	757.354	182.239
0.3	734.997	175.738
0.4	703.558	166.579
0.5	659.046	155.125
0.6	597.468	141.161
0.7	514.834	123.896
0.8	407.152	101.961
0.9	270.432	73.410
1.0	100.681	35.716

Table 4.1: First twelve significant free vibration periods (Sec) of BMP dam models

Mode no.	For RF model	For FF model
1	0.8773	1.1957
2	0.8555	0.9343
3	0.6228	0.8068
4	0.5637	0.7031
5	0.5485	0.6728
6	0.5030	0.6318
7	0.4955	0.6060
8	0.4815	0.5713
9	0.4626	0.5557
10	0.4467	0.5414
11	0.4330	0.5172
12	0.4244	0.4981

Table 4.2: Vertical displacement (mm) data along a vertical line through BMP dam core-centre, under gravity turn-on load

Height above the base (m)	For RF model	For FF model
0.0	0.000	20.512
11.7	54.292	74.981
23.4	109.609	130.774
35.1	161.411	184.314
46.8	207.397	234.106
58.5	246.634	278.562
70.2	278.145	316.520
81.9	300.652	346.444
93.6	309.391	364.512
105.3	289.533	358.441
117.0	197.415	288.525



Table 4.3: Vertical displacement (mm) data along a horizontal line at the height of 93.6 m above the base of core, under gravity turn-on load.

Distance from centre in m (+ distance towards right)	For RF model	For FF model
-16.70	130.352	192.202
-13.36	188.404	247.225
-10.02	241.441	296.495
-6.68	279.088	332.929
-3.34	301.998	355.931
0.00	309.391	364.512
3.34	301.420	358.531
6.68	277.986	338.063
10.02	239.890	304.014
13.36	186.647	256.850

Table 4.4: Rayleigh - damping coefficients calculated

Model		
RF	0.060938	0.026737
FF	0.212111	0.030379

Table 5.1: Peak horizontal crest acceleration of the history

Model definition	Acceleration, in units of g
RF_WOR	0.69
FF_WOR	0.68
RF_WR	0.96
FF_WR	0.51

Table 5.2: Permanent settlement results for the BMP dam models

Model definition	Permanent Crest Settlement, m
RF_WOR	0.89
FF_WOR	0.88
RF_WR	1.20
FF_WR	0.56

## APPENDIX C

### CALCULATIONS FOR HYDRODYNAMIC EFFECTS

According to IS guidelines [22], the hydrodynamic added pressures (Zangar, 1952) are given by:

$$p_{hd} = C \frac{a_{max}}{g} \gamma_w h$$

$C$  = hydrodynamic pressure coefficient, which is the function of angle and depth below water surface ( $y/h$ ), and is read from the chart given in figure C.1.

$\gamma_w$  = unit weight of water

$h$  = height of water surface above the base of the dam

$g$  = acceleration due to gravity

$a_{max}$  = design PHGA at the elevation of the toe of the dam

In the absence of site specific estimates of design peak horizontal ground acceleration, the following estimate is recommended.

$$\frac{a_{max}}{g} = Z I S$$

$Z$  = Zone Factor given in IS: 1893-Part 1 (2002)

$I$  = Importance factor, given in the guideline [22]

$S$  = empirical coefficient to account for the amplification of ground motion between bedrock and the elevation of the toe of the dam, given in the guideline [22]

Using the notations  $z$  = height above the base,  $p(z)$  = hydrodynamic pressure at a height  $z$  above the base; the hydrodynamic added force to be lumped at a node with tributary area between heights  $z_1$  and  $z_2$  is given by

$$F(z_1 - z_2) = \int_{z_1}^{z_2} p(z) dz$$

Again equating the hydrodynamic force to the equivalent virtual inertial force of the reservoir, the shape of the body of the reservoir  $b(z)$  that is assumed to be associated with the dam may be evaluated. That is,

$$p(z) \cdot dz = dM \cdot a_{\max} = dV \cdot \gamma_w \cdot a_{\max} = dA \cdot \gamma_w \cdot a_{\max} = b(z) \cdot dz \cdot \gamma_w \cdot a_{\max}$$

$$\text{Or, } C(z) \frac{a_{\max}}{g} \gamma_w h = b(z) dz \frac{\gamma_w}{g} a_{\max} ; \text{ since } \gamma_w = \frac{\gamma_w}{g}$$

$$\text{Or, } b(z) = C(z) \cdot h$$

Thus the hydrodynamic added mass to be lumped at a node having tributary area between heights  $z_1$  and  $z_2$  is given by,

$$M(z_1 - z_2) = \int_{z_1}^{z_2} b(z) \gamma_w dz$$

Following the aforementioned guide, the following values are obtained for the cores of BMP dam.

$$= \tan^{-1}(0.5/1) = 26.56^\circ$$

From figure C.1, C for different depths is read.

The plot of C against z is shown in figure C.2.

$$Z = 0.36$$

$$I = 2$$

$$S = 1$$

$$\text{So, } \frac{a_{\max}}{g} = 0.72$$

$$\gamma_w = 9.81 \text{ kN/m}^2$$

$h = 115 \text{ m}$  for main dam-core (approximately taken 117 m to lump the top hydrodynamic added value at the crest node since the resulting effect is negligible in the present high dam case).

$h = 57 \text{ m}$  for coffer dam core (The head above the crest is assumed to contribute only to static water pressure and to have negligible effect in hydrodynamic added values)

The plots of  $p(z)$  and  $b(z) \gamma_w$  for main dam core and coffer dam core are presented in figure C.3a, figure C.3b, figure C.4a and figure C.4b respectively.

From the plots, the regression equations are derived as:

$$p(z) = -3 \times 10^{-6} z^4 + 0.0006 z^3 - 0.056 z^2 + 0.4443 z + 470.65; \text{ for main dam core}$$

$$p(z) = -3 \times 10^{-5} z^4 + 0.0023 z^3 - 0.1149 z^2 + 0.4443 z + 229.29; \text{ for coffer dam core}$$

$$b(z)_w = -0.035 z^3 + 0.279 z^2 - 115.6 z + 66885; \text{ for main dam core}$$

$$b(z)_w = -0.004z^4 + 0.331 z^3 - 16.26 z^2 + 62.89 z + 32463; \text{ for coffer dam core}$$

Then, the hydrodynamic forces and hydrodynamic added masses are computed. These are lumped at the upper limit tributary node in present work. The calculated values are given in table 3.3 and table 3.4 respectively.

## APPENDIX D

### CALCULATIONS FOR PHREATIC LINE

The symbols used in the calculations are as per reference 37 and dimensions are in meters. Figure D.1 also demonstrates the notations.

Information about the core of main dam:

Crest width = 10 m

Side slopes = 0.5 H: 1V

Height of core above base = 117

Reservoir level above base = 115

The equation of basic parabola with origin at focus, F (downstream toe):

$$\sqrt{(x^2 + y^2)} = x + y_0$$

$$\text{Or, } r = \frac{y_0}{(1 + \cos u)}$$

$y_0$  = distance of focus from the directrix

The co-ordinates of point A' on the upstream face of core = (69.5, 115)

$m = 57.5$ ;  $0.3 \text{ m} = 17.25$

Thus, the co-ordinates of point A, the first point on basic parabola = (86.75, 115)

Using this point, value of  $y_0$  is determined. This gives  $y_0 = 57.30$

Now, for the point E on the basic parabola on the downstream face of core,

$$\theta = \tan^{-1}(1/0.5) = 63.47^\circ$$

So,  $r_E = 103.67 = a + \frac{a}{\cos \theta}$

For earth dams, correction is required. Point A on upstream face and point D on downstream face are the corrected points on the phreatic line. According to the A. Casagrande's correction (chart referred from reference 37), for  $\theta = 63.47^\circ$ ,

$$\frac{\Delta a}{a + \Delta a} = 0.31 \Rightarrow a = 71.53 \text{ meters}$$

Thus, the y-ordinate of point D =  $71.53 \sin \theta = 64$  meters  $\approx 0.55$  x height of core.

The remaining curve is located by eye judgment such that the curve is normal to the upstream face at A and tangent to the downstream face at D.